aaquetzalli is required for epithelial cell polarity and neural tissue formation in *Drosophila*

Miguel A Mendoza-Ortíz [1] , **Juan M Murillo-Maldonado** [1] , **Juan R Riesgo-Escovar** Corresp. [1]

[1] Developmental Neurobiology and Neurophysiology, Instituto de Neurobiología, Universidad Nacional Autónoma de México, Querétaro, Querétaro, México

Corresponding Author: Juan R Riesgo-Escovar
Email address: juanriesgo@prodigy.net.mx

Morphogenetic movements during embryogenesis require dynamic changes in epithelial cell polarity and cytoskeletal reorganization. Such changes involve, among others, rearrangements of cell-cell contacts and protein traffic. In *Drosophila melanogaster*, neuroblast delamination during early neurogenesis is a well-characterized process requiring a polarized neuroepithelium, regulated by the Notch signaling pathway. Maintenance of epithelial cell polarity ensues proper Notch pathway activation during neurogenesis. We characterize here *aaquetzalli* (*aqz*), a gene whose mutations affect cell polarity and nervous system specification. The *aqz* locus encodes encodes a protein that harbors a domain with significant homology to a proline-rich conserved domain of nuclear receptor co-activators. *aqz* expression occurs at all stages of the fly life cycle, and is dynamic. *aqz* mutants are lethal, showing a disruption of cell polarity during embryonic ventral neuroepithelium differentiation resulting in loss of epithelial integrity and mislocalization of membrane proteins (shown by mislocalization of Crumbs, DE-Cadherin, and Delta). As a consequence, *aqz* mutant embryos with compromised apical-basal cell polarity develop spotty changes of neuronal and epithelial numbers of cells.

1   **TITLE:**

2   *aaquetzalli* is required for epithelial cell polarity and neural tissue formation in *Drosophila*

7   **AUTHORS:**

8   Miguel A. Mendoza-Ortiz[a], Juan M. Murillo-Maldonado[a] & Juan R. Riesgo-Escovar[a]#.

10   Developmental Neurobiology and Neurophysiology, Instituto de Neurobiología, Universidad

11   Nacional Autónoma de México, Querétaro, Querétaro, México.

15   # Corresponding author: Juan R. Riesgo-Escovar: juanriesgo@prodigy.net.mx

23 **Abstract**

25 Morphogenetic movements during embryogenesis require dynamic changes in epithelial cell

26 polarity and cytoskeletal reorganization. Such changes involve, among others, rearrangements of

27 cell-cell contacts and protein traffic. In *Drosophila melanogaster*, neuroblast delamination

28 during early neurogenesis is a well-characterized process requiring a polarized neuroepithelium,

29 regulated by the Notch signaling pathway. Maintenance of epithelial cell polarity ensues proper

30 Notch pathway activation during neurogenesis. We characterize here *aaquetzalli* (*aqz*), a gene

31 whose mutations affect cell polarity and nervous system specification. The *aqz* locus encodes

32 encodes a protein that harbors a domain with significant homology to a proline-rich conserved

33 domain of nuclear receptor co-activators. *aqz* expression occurs at all stages of the fly life cycle,

34 and is dynamic. *aqz* mutants are lethal, showing a disruption of cell polarity during embryonic

35 ventral neuroepithelium differentiation resulting in loss of epithelial integrity and mislocalization

36 of membrane proteins (shown by mislocalization of Crumbs, DE-Cadherin, and Delta). As a

37 consequence, *aqz* mutant embryos with compromised apical-basal cell polarity develop spotty

38 changes of neuronal and epithelial numbers of cells.

42 **Introduction**

44 Cell polarity is a crucial crossroads for epithelial development and function. Epithelial

45 polarization generates and maintains differentiation of apical and basolateral membrane domains.

46 In fruit fly embryos, cellularization and cell polarity come first and preempt gastrulation and

47 further development (Campos-Ortega and Hartenstein, 1997). Cellular blastoderm fly embryos

48 exhibit cell polarization (Nusslein-Volhard and Wieschaus, 1980). For this, both membrane-

49 attached and cytosolic cytoskeletal proteins are required. Failure of proper polarization leads to

50 early death with a very early phenotype during cellularization and/or germband extension (Pai et

51 al., 1996; Peifer and Wieschaus, 1990; Tepass et al., 1996).

52

53 Once attained, cellular polarization must be regulated and maintained (Campos-Ortega and

54 Hartenstein, 1997). A well-studied case is neurulation in the fly. The embryonic tissue that gives

55 rise to both fly neural and skin precursors is the ventral ectoderm, or neuroectoderm (Campos-

56 Ortega and Hartenstein, 1997; Campos-Ortega and Knust, 1990). Early positional cues establish

57 the neuroectodermal region in the procephalon and the ventrolateral ectoderm (Egger et al.,

58 2008; Technau et al., 2006). Within this epithelial sheet, initially equivalent groups of cells, the

59 proneural groups, form, evidenced by expression of marker genes, like the basic-helix-loop-helix

60 (bHLH) *achaete-scute* complex and molecules of the Notch (N) signaling pathway. Among these

61 cells, Notch signaling limits the number of neural precursors that delaminate and form

62 neuroblasts (Bertrand et al., 2002; Campos-Ortega and Knust, 1990; Cornell and Ohlen, 2000;

63 Hartenstein et al., 1992; Portin, 2002; Skeath et al., 1992; Technau et al., 2006; Zhao et al.,

64 2007). From each individual proneural cluster, normally just one cell differentiates as a

65 neuroblast (Cabrera, 1990; Fortini, 2009; Fortini and Artavanis-Tsakonas, 1993; Schrons et al.,

66 1992). Neuroblasts migrate and divide to give rise to ganglion mother cells, and ultimately, to

67 neurons and glia (Karcavich, 2005; Zhong and Chia, 2008). Non-selected cells receiving the

68 Delta signal remain in the ectoderm and become epidermoblasts, differentiating into skin cells

69 (Hartenstein and Wodarz, 2013; Portin, 2002). The process necessitates maintenance of polarity

70 and changes in cell shape (Harris and Tepass, 2008; Harris, 2012; Wang et al., 2004).

71

72 Recent studies show that cell polarity regulatory proteins (CPRPs), such as Cdc42, Par complex

73   components, and WASP proteins establish apical-basal cell polarity (Bayraktar et al., 2006;
74   Harris and Tepass, 2008; Krahn and Wodarz, 2009; Tepass, 2012). Epithelial defects like loss of
75   cell dissociation and apical-basal polarization affect adherens junctions (AJ), and the way in
76   which Dl and N interact (Buszczak et al.). Membrane polarization and Dl activation are critical
77   events during early neurogenesis (Bayraktar et al., 2006; Fehon et al., 1991; Harris and Tepass,
78   2010; Kooh et al., 1993; Liu et al., 2012; Weinmaster and Fischer, 2011). Disrupted CPRPs alter
79   epithelial integrity and cause abnormalities in neuroblast proliferation and morphogenetic
80   movements during early neurogenesis. This may result in nervous system hyperplasia paralleled
81   by loss of epidermis, a typical "neurogenic" phenotype (Bayraktar et al., 2006; Harris and
82   Tepass, 2008; Harris and Tepass, 2010; Krahn and Wodarz, 2009; Wang et al., 2004;
83   Weinmaster and Fischer, 2011).
84
85   Here we characterize the *aaquetzalli* (*aqz*) gene, which encodes several alternatively spliced
86   transcripts expressed throughout the life cycle. *aqz*, meaning 'fan' in nahuatl, and the name
87   refers to the abnormal embryonic cuticular phenotypes of mutant embryos. Mutations in *aqz* are
88   lethal, with an extended phenocritical period. Previous studies suggest that *aqz* is required
89   pleiotropically during *Drosophila* embryogenesis: *aqz* mutant germline clones die with cuticular
90   holes (Perrimon et al., 1996), and *aqz* RNAi injected in developing embryos show axon guidance
91   and synaptogenesis defects (Ivanov et al., 2004). These mutant phenotypes are in ectodermally
92   derived cells (epidermis and nervous tissue), despite affectation in all cells in the first case, and
93   generalized injection of RNAi in developing embryos in the second case. So, these experiments
94   support the tenet that *aqz* is required in ectodermal tissues.
95
96   In order to fully characterize the locus, we generated and identified new mutant *aqz* alleles.
97   These alleles show new, more generalized zygotic neural and epidermal mutant phenotypes
98   similar to N pathway mutants ("neurogenic" phenotypes). *aqz* is expressed early in the ectoderm
99   and ectodermally derived tissues. Our findings describe and establish an early role for *aqz* in
100 ectoderm differentiation as a modulator of cell polarity, promoting apical polarization to
101 maintain epithelial integrity. *aqz* modulates Dl membrane localization during neural lateral
102 inhibition.
103

104   **Materials & Methods**

105

106   **Fly strains, genetics and husbandry**

107   Flies were housed in standard conditions (25ºC, 12:12 light:dark cycles and 50% humidity) in

108   standard food vials (unrefined sugar-baker's yeast-agar-gelatin-water). Oregon R and *yw* were

109   used as control stocks. aqz^2, aqz^6, and aqz^7 are lethal insertion alleles. aqz^2 is Bloomington stock

110   #14691 (y^1 w^{67c23}(y^1 w^{67c23}; P{y[+mDint2] w[BR.E.BR]=SUPor-P}KG08159 ry^{506}); aqz^6 is

111   Bloomington stock # 20315 (*y1 w67c23; P{EPgy2}CG9821EY11495*). aqz^7 was a lethal

112   insertion line that is now lost (former Bloomington stock #1492). aqz^{GFP} is also a transposon

113   insertion, and was stock #CB03335 from the former FlyTrap Stock Collection at Yale

114   University, USA. It is a lethal insertion that generates chimeric proteins GFP::Aqz. New *aqz*

115   alleles generated: aqz^1, aqz^3 and aqz^5, are excision events. aqz^3 is an excision event from the now

116   lost aqz^7 insertion. aqz^1 and aqz^5 are excisions from aqz^2. All excision alleles are lethal.

117

118   aqz^{rescue} was generated by transgenesis using P[acman] BAC #CH322-25015 (Venken et al,

119   2009). CH322-25015 has approximately a 19 Kb fly genomic fragment from 4631615 to

120   4650999 on chromosome three, including the complete *aqz* locus (CG9821), CG9836 or *IscU*,

121   *iron sulfur cluster assembly enzyme,* where the known mutants alleles die between late larval

122   life and pupariation, CG8369 (an undescribed Kazal domain containing protein), CG9837 and

123   CG8359, or *hng2*, *hinge2*, plus a lncRNA: CR43130, that partially overlaps CG9821, but in the

124   opposite orientation. The whole genomic rescue construct was inserted on 2R by recombineering

125   at 53B2 (using Bloomington line #9736). We also used three different deficiencies that uncover

126   the *aqz* locus to perform complementation tests: Bloomington stock #7629 (w^{1118};

127   *Df(3R)Exel6150,   P{XP-U}Exel6150/TM6B, Tb^1*);   Bloomington   stock   #24982   (w^{1118};

128   *Df(3R)BSC478/TM6C, Sb^1 cu^1*), and Bloomington stock #25010 (w^{1118}; *Df(3R)BSC506/TM6C,*

129   *Sb^1 cu^1*).

130

131   ***in situ* hybridization**

132   Embryo *in situ* hybridization was done following (Tautz and Pfeifle, 1989), with few

133   modifications for fluorescence detection. Briefly, whole embryos were fixed with formaldehyde,

134   and hybridized with digoxigenin RNA probes overnight at 55ºC in hybridization buffer. *aqz* 5'

135   RNA probes (derived from clone LD47990, which corresponds to the 5' end of *aqz*, sense and

136   anti-sense) were synthesized using Roche's digoxigenin RNA labeling kit following the

137   manufacturer´s protocol (Roche, Switzerland). The fixed and hybridized embryos were incubated

138   with polymerized HRP-conjugated anti-digoxigenin antibody at a 1:2000 dilution for 1 hr 45 min

139   at room temperature, washed and incubated with 1:10 diluted Tiramidine-CY3 for 45 min, using

140   the tyramidine derivative system (TSA, Perkin Elmer, USA), and mounted in Vectashield

141   (Vector Laboratories, USA).

142

143   **Northern blot analysis**

144   Total RNA was isolated from 8-12 hr old embryos, 2nd and 3rd instars larvae, pupae, and adults

145   with Trizol, according to the manufacturer's instructions (Gibco/BRL, USA). Northern blotting

146   was done according to standard procedures (Sambrook et al., 1989). Approximately 3-4

147   micrograms of total RNA was loaded per lane. DNA probes were from cDNA clone LD47990

148   (Stapleton et al., 2002), for the *aqz* 5' region, which is common to all *aqz* transcripts, and clone

149   LD02090, which labels the 3' end of the gene not present in *aqz* RA, but present in *aqz* RB, RC,

150   and RD. The probes were labeled with a-^{32}P deoxycytidine 5'-triphoshpate, following Feinberg

151   and Vogelstein (1984). Both cDNA clones were purchased from the Berkeley Drosophila

152   Genome Project clone collection.

153

154   **Antibody generation**

155   A rabbit polyclonal antiserum was generated against the KSIRLKKGAC peptide, representing

156   the Aqz amino terminus. Immunoglobulins G (IgGs) were affinity purified from immune serum

157   (New England Peptide, MA, USA). This antibody failed to detect Aqz proteins in Western blots,

158   but detectd Aqz in tissue sections.

159

160   **Western blot**

161   Embryos were homogenized and immunoblotted following (Wodarz, 2008). Proteins were

162   separated on 10% denaturing acrylamide gels (SDS-PAGE), transferred to nitrocellulose

163   membranes and incubated with rabbit anti-GFP (1:5000, SC-8334, Santa Cruz Biotechnology,

164   USA) as primary antibody. We pre-absorbed anti-GFP before use by incubating diluted primary

165   antibody with wild type fixed embryos in incubation solution overnight. We used Alkaline

166   Phosphatase (AP)-conjugated secondary antibodies (goat anti-rabbit 1:1000 from ZYMED).

167   Secondary antibody was incubated for 1 hour at room temperature. We used the NBT/BCIP

168   substrate solution (Roche Diagnostics) for AP detection.

169

170   **Immunohistochemistry**

171   We followed the embryo staining protocol in (Karr and Alberts, 1986), except for aqz^{GFP}

172   embryos. The aqz^{GFP} embryos were washed in methanol only once, and rehydrated immediately.

173   For primary antibodies, we used rat anti-Deadpan (1:2, gift of Cheng-Yu Lee), rabbit polyclonal

174   anti-Aqz (1:500 this work), and rabbit anti-GFP (1:100, SC-8334, Santa Cruz Biotechnology,

175   pre-absorbed with wild type embryos in incubation solution overnight before use). Polyclonal rat

176   anti-Elav (7E8A10, 1:250), polyclonal rat anti-DE-cad (DCAD2, 1:10), mouse monoclonal anti-

177   FASIII (7G10, 1:100), mouse monoclonal anti-EVE (3C10, 1:10), mouse monoclonal anti-

178   Coracle (C615.16, 1:250), mouse monoclonal anti-22C10 (1:200), mouse monoclonal anti-

179   BP102 (1:200), mouse monoclonal anti-Repo (8D12, 1:200), mouse monoclonal anti-Dl

180   extracellular domain (C594.9B, 1:100), mouse monoclonal anti-Crumbs (Cq4, 1:100), and

181   mouse monoclonal anti-Dlg (4F3, 1:3) were from the Developmental Studies Hybridoma Bank,

182   University of Iowa, Iowa City, USA. Primaries were incubated with fixed embryos overnight at

183   4ºC. Embryos were then washed 4 times for 20 minutes each using 0.3% Triton X-100 in PBS.

184   Anti-Deadpan, anti-Aqz, anti-Eve, anti-DE-cadherin, anti-GFP and anti-Delta antibody signals

185   were amplified using biotin-conjugated secondary antibodies in combination with the Vector

186   Elite ABC kit (Vector Laboratories, Calif.) according to the manufacturer's instructions.

187   Fluorescent-coupled (1:1000, ZYMED) and biotin-conjugated secondary antibodies (1:500,

188   Santa Cruz Biotechnology) were incubated for 2 hours at room temperature. For embryos

189   incubated with biotin-conjugated antibodies, we used the dye-labeled tyramidine derivative

190   system (TSA) for signal amplification. After washing 4 times with 0.3% Triton X-100 in PBS,

191   fluorescently labeled embryos were mounted in Vectashield.

192

193   **Cuticle preparations**

194   We followed the protocol described by (Nüsslein-Volhard and Wieschaus, 1980). Embryos and

195   1st instar larvae were collected 24 hours after egg laying, dechorionated in 50% bleach for 5

196   minutes, rinsed in distilled water and placed in an Eppendorf tube containing 50% heptane and

197   50% methanol, and shaken vigorously for 2 minutes. The upper phase was removed and both

198   embryos and 1st instar larvae were washed with 100% methanol 3 times. Embryos and 1st instar

199   larvae were rehydrated with PBT (PBS + 0.3% Triton X-100). Once rehydrated, they were

200   carefully dropped onto a glass slide and covered with mounting medium (Hoyer's Medium or

201   PVA) and coverslipped. They were incubated at least one day in a hot plate. Cuticles were

202   visualized using dark field microscopy.

203

204   **Embryonic lethality**

205   To assess embryonic lethality, we separated and collected aqz^{GFP} homozygote eggs from 24

206   hours egg-laying plates under a dissecting microscope equipped with a blue light source and a

207   GFP filter. Homozygote mutant embryos fluoresce with GFP, and can be distinguished from

208   control (non-fluorescent) or heterozygous (weakly fluorescent) eggs. These were placed on fresh

209   egg-laying plates alongside wild type, control Oregon R eggs from the same day, and incubated a

210   further 72 hours. At the end, non-hatching, dead embryos were counted.

211

212   **DNA sequencing**

213   Automated sequencing was performed using an ABI 310 sequencer. We sequenced fully cDNAs

214   SD19655, LD74990, RE74095, LD18978 and LD02060. For aqz^{1}, we selected homozygous

215   mutant embryos by lack of GFP expression present in the balancer chromosome, and made a

216   crude homogenate from them, to use for PCR amplification. We PCR-amplified using primers

217   AqzA (TACACCACCGTCTATTGCG) and AqzB (CCCCATTGTGTCAGATTTCTT),

218   amplifying the *aqz* promoter region for aqz^{1}. We cloned the ensuing PCR products in pGEMT

219   Easy vector (Promega, USA). The PCR product inserts were sequenced fully. We sequenced

220   three independent mutant clones, and all confirmed the mutation in the promoter region of aqz^{1}.

221

222   **Genetic assays**

223   Crosses or stocks were let to lay eggs in agar plates, and eggs laid were collected, classified, and

224   counted. We selected stage 14-15 embryos (late neurogenesis). Embryos were fixed and stained

225   using anti-Elav (NS) and anti-Coracle (epidermis), to score neurogenic phenotypes. The

226   percentage of embryos with wild type (WT, no defects in the NS and epidermis) or "neurogenic"

227   phenotype was calculated by using the following formula: % of WT or neurogenic embryos =

228   WT or neurogenic embryos/ total of homozygotes embryos counted*100. Fisher's exact test was

229   used to assess significance of the differences indicated. We scored at least 400 embryos for every

230   experiment.

231

232   **aqz rescue experiments**

233   To rescue aqz in an endogenous genomic context that includes the whole locus and alternatively

234   spliced transcripts, we used a genomic BAC (#CH322-25015) that has a genomic insert of 19,

235   384 bp in the attB-P[acman]-CmR-BW vector, roughly centered on CG9821 encompassing the

236   whole locus, but including four other neighboring genes (CG9836, CG8369, CG9837, and

237   CG8359, plus a lncRNA: CR43130, that partially overlaps the aqz sequence in the opposite

238   orientation). These other loci, excepted aqz, have no known lethal alleles. Of these, only *IscU*

239   (CG9836) and *hng2* (CG8359), besides aqz, are expressed significantly during embryogenesis

240   (there is mid- to late embryonic expression of CG9837) (Dos Santos et al., 2015). Mutant alleles

241   or insertions in these loci (stocks # 22145, 34193, 31835, 14691) behave differently from aqz^{GFP},

242   as they fully complement the *Df(3R)Exel6150* that is embryonic lethal over aqz^{GFP}, and not

243   surprisingly fully complement aqz^{GFP} as well (supplementary table 1). We inserted this genomic

244   construct, thereafter called aqz^{RESCUE} construct, by standard methods at a attB acceptor site at

245   53B2, as stated above. This insertion has no phenotype in a wild type background. We then

246   constructed stocks aqz^{RESCUE}; aqz^{mutant} and controls that were doubly balanced with the

247   T(2:3)*CyO-TM3,Ser,GFP* fused chromosome two and three balancers (Bloomington stock

248   #5703). Homozygous mutants either with one or two copies of the aqz^{RESCUE} construct were

249   assessed for rescue both by staining embryos as above for neurogenic phenotypes, and for adult

250   viability. For adult viability, homozygous mutant embryos and controls with and without rescue

251   construct present were collected from egg lays, allowed to develop, and emerging adults were

252   scored. Fisher's exact test was used to assess significance of the differences.

253

254   **Image acquisition and processing**

255   We studied embryos using light, fluorescence, and laser scanning confocal microscopy (LSM).

256   Cuticles and immunofluorescence of whole embryos were imaged using a digital camera

257   (CoolSnap, Photometrics, USA) on a Nikon E600 Eclipse microscope with Plan-Fluor 20X/0.50

258   NA and a Nikon Super High Pressure Mercury Lamp. Confocal sections of embryos were made

259 in a Zeiss LSM 510 Meta with Plan-Neofluar 25x/0.8 NA and a Plan-FLUAR 100X/1.45 NA

260 objectives (Carl Zeiss), or a Zeiss LSM 780 with Plan-APOCHROMAT 25X/0.8 NA and Plan-

261 APOCHROMAT 63X/1.40 NA objectives (Carl Zeiss) at 18ºC. For cuticle and fluorescence

262 image processing, we use iVision 4.0.12 software (BioVision Technologies, 2008). Confocal

263 sections were processed using the Image Browser software (Carl Zeiss) used to generate image

264 stacks. All captured images were processed using Adobe Photoshop software.

265

266 **Ribosome footprinting, mRNA-seq, sequence visualization and alignment.**

267 We used raw data generated and publish by (Dunn et al., 2013) available in NCBI's Gene

268 Expression Omnibus (Edgar et al., 2002) under GEO series accession number GSE49197

269 (http://www. ncbi.nlm.nih.gov/geo/query/acc.cgi?acc=GSE49197). We used the Integrated

270 Genome Browser (IGB) software for visualization and exploration of the *aqz* genome locus and

271 corresponding annotations (Nicol et al., 2009).

272

273 **Results**

274

275 **The *aqz* locus**

276 The isolated *aqz* transposon insertions map to a locus (CG9821 in Flybase) at 85B2 on the right

277 arm of the third chromosome. This locus has alternative splicing at the end of the first exon and

278 different 3' ends, as judged from ESTs from the locus, and gives rise to at least three different

279 transcripts differing in size and composition (Fig. 1A, C (Dos Santos et al., 2015)). The CG9821

280 locus spans over 7Kb, partially overlapping a non-coding RNA gene at its 5' end (CR43130). It

281 also overlaps CG9837 at its 3' end (at least 89 bp of the 3' end of CG9821 overlap the CG9837

282 5' end). CG9837 is transcribed in the same direction as CG9821. The 5' end of CG9821 has a

283 proline-rich domain found in nuclear receptor co-activators (PNRC-domain proteins), present in

284 invertebrate and vertebrate proteins (Fig. 1B).

285

286 ***aqz* cDNAs and proteins**

287 We identified and sequenced cDNAs and genomic fragments from the *aqz* locus. There is a

288 wealth of ESTs isolated from the CG9821 region, consistent with widespread expression. We

289 sequenced fully several of these ESTs and pieced them together with other sequences available.

290   The two exons composing the transcribed part of the locus vary in size, due to alternative

291   splicing in the first exon and different endings of the second exon (Fig. 1A).

292

293   The Aqz protein harbor a domain with significant homology to a proline-rich conserved domain

294   of nuclear receptor co-activators (PNRC-domain proteins; Fig. 1B). This conserved domain, a

295   proline rich, SH3 protein-protein interaction domain thought to mediate union to several nuclear

296   receptors in vertebrates, is present in both vertebrate and invertebrate proteins, and is 60 aa long.

297   Within it, a YAG motif besides several proline residues and two more carboxy-terminus-located

298   small regions of homology constitute the conserved core of the domain. Vertebrate proteins are

299   thought to interact with nonsense-mediated RNA decay proteins (Lai et al., 2012), as well as

300   with a variety of nuclear receptors. Knock out mice for PNRC2 are viable and fertile, but males

301   exhibit a lean phenotype due to higher energy expenditure (Zhou et al., 2008). Whether fly

302   proteins also exhibit similar binding and functional roles is as yet unclear. *Drosophila*

303   *melanogaster*, among sequenced Drosophila species, possesses a second uncharacterized protein

304   with this motif: CG32797 (Fig. 1B), mutations in which may have similar phenotypes to those

305   encountered in mice PNCR2 knockouts. It remains to be seen whether any Aqz mutant has

306   higher energy expenditure, or similar phenotypes to the PNCR2 knockouts.

307

308   The theoretically reconstructed cDNAs are somewhat at variance from data published for

309   CG9821 and CG9837 (St Pierre et al., 2014). cDNAs predicted for CG9821 are shorter than the

310   ones we pieced together, but the annotations do not take into consideration several ESTs located

311   towards the 3' end of CG9821, also reported, that partially overlap other identified ESTs for

312   CG9821 and CG9837 (Fig. 1A; supplementary Fig. 1), and the RNAseq data posted from the

313   modEncode project, which shows that the two annotated loci overlap (Celniker et al., 2009).

314   There are four predicted different isoforms for CG9821 mRNAs, all with the same coding

315   sequence, two of which are very similar in size (*aqz-RD* and *aqz-RB*), varying only in the size of

316   the first exon (cDNAs of 4950 and 4719 nucleotides long, respectively). The size of the shortest

317   predicted cDNA isoform (*aqz-RA*) is just 2357 nucleotides long. The longest predicted cDNA

318   (*aqz-RC*) is approximately 6145 nucleotides long and it overlaps at least 89 bp with the CG9827

319   locus (Fig. 1A).

320

321 In order to contrast these reconstructions and annotations from ESTs and gene-prediction
322 software (Celniker et al., 2009), we performed Northern blots. We identified in Northern blots
323 with 5' probes at least three differently sized mRNAs that correspond roughly in size to the ones
324 we reconstructed, two of which are expressed throughout the fly life cycle (Fig. 1C). This last
325 agrees well with published data showing *aqz* expression at all life cycle stages and in multiple
326 tissues including the brain, ovary, imaginal discs, and larval salivary glands (Jagadeeshan and
327 Singh, 2005; St Pierre et al., 2014).

328

329 We observe a darker band at slightly over 5 Kb, that may correspond to the two 4.9 and 4.7
330 bands annotated for CG9821. We observe a fainter larger band at 7.5 Kb; this last may
331 correspond to the longest reconstructed cDNA spanning CG9821 and overlapping CG9837. We
332 also observe a smaller band at 3.1 Kb with a 5' probe; the closest annotated CG9821 mRNA is
333 2.35 Kb long. This smaller mRNA species is only seen in adult flies with a 5' probe, and not
334 with a more 3' probe, showing that the small cDNA comes from the 5' end of the locus, as
335 predicted for the 2.35 Kb species. These cDNAs share the same 5' end harboring the PNRC
336 domain, but have different 3' extensions (Fig. 1C). These extensions are mostly predicted as
337 non-coding (St Pierre et al., 2014). Since the 5' coding sequence is common for the cDNAs, we
338 generated an antibody against an Aqz amino terminal peptide fragment. Unfortunately, we were
339 not able to obtain a clear and specific signal using this antibody in Western blots.

340

341 We also analyzed ribosome occupancy data published for the locus, using data from a modified
342 protocol of ribosome profiling assay. This assay has helped reveal that stop codon read-through
343 plays an important regulatory role in N-terminally and C-terminally protein extension during
344 mRNA translation (Dunn et al., 2013). We performed an *aqz* mRNAs ribosome footprint
345 analysis using RNA abundance and ribosome density data generated and published (Dunn et al.,
346 2013), available at NCBI GEO (http://www.ncbi.nlm.nih.gov/geo/), and viewed the display
347 alignments using the Integrated Genome Browser 8.1 (IGB) sequence viewer software (Fig. 2).
348 The analysis reveals that the first exon is transcribed as well as infrequent 3' extensions in the
349 second exon, beyond the predicted stop codon. These data are consistent with our Northern
350 results (Fig. 1C).

351

352 **_aqz_ alleles**

353 We identified and generated new _aqz_ alleles. Two previously described mutant alleles appear to

354 be weak loss-of-function alleles (named here _aqz²_ (also known as P14691), an insertion in the

355 promoter, and _aqz⁷_ (also known as P1492), an insertion in an intron, now lost (Perrimon et al.,

356 1996); Fig. 1A). We generated imprecise excision lines. Mutant embryos have zygotic

357 embryonic mutant phenotypes affecting the central NS and the cuticle (supplementary Fig. 2).

358 The RNAi study referred to above also pointed to an _aqz_ requirement in axon guidance and

359 synaptogenesis (Ivanov et al., 2004).

360

361 The new alleles generated by imprecise excisions are lethal, and from these we characterized

362 _aqz¹_ further. Molecular analysis of _aqz¹_ revealed a 4 bp insertion in the promoter region of

363 CG9821 (sequence inserted: ACAT, 189 bp 5' from the transcription start site, and 171 bp 5'

364 from the parental P transposon insertion), probably due to the imprecise P-element excision

365 event (Fig. 1A). This 4 bp insertion is not present in control strains, in other _aqz_ mutants, or in

366 revertants from the same P-element excision experiment.

367

368 We also identified another lethal allele, _aqz^{GFP}_, from a collection of gene traps in the former

369 Yale Gene Trap stock center (Kelso et al., 2004). This allele, _aqz^{GFP}_, has an insertion in the first

370 intron/first exon (depending on the splice variant), coding for GFP, theoretically giving rise to a

371 chimeric protein made of GFP fused to the Aqz amino terminus (GFP::Aqz). As shown in Fig.

372 1D, we detected only one band of approximately 40 kDa in Western blots from _aqz^{GFP}_

373 homozygous mutant embryos using an anti-GFP antibody. This band must contain GFP (of

374 approximately 26.9 kDa), and a fragment of the Aqz protein product (of approximately 13 kDa).

375

376 In order to genetically characterize the _aqz_ locus, we conducted complementation tests of lethal

377 mutant alleles. The _aqz¹_ and _aqz²_ alleles complement each other and three different deficiencies

378 uncovering the locus. These mutant alleles also complement the _aqz^{GFP}_ allele. In contrast, _aqz^{GFP}_

379 does not complement the same three different deficiencies that uncover the locus, effectively

380 mapping _aqz^{GFP}_ to the common interval uncovered by them at 85B, where the _aqz_ locus, and the

381 insertion points of _aqz^{GFP}_ and the other _aqz^{insertions}_, lie (for example, _aqz²_ and _aqz^{GFP}_ lie only 322

382 bp apart within the promoter/first exon/intron of the locus), yet they complement (Fig. 1A; Table

383   1). The fact that aqz^1 complements the three deficiencies used (that do not complement aqz^{GFP})

384   and aqz^{GFP} could also be explained saying that the lethality of aqz^1 maps elsewhere, despite the

385   molecular lesion and similar mutant phenotypes. All aqz mutants, despite their origin, have the

386   same mutant phenotypes. In all, a fraction of mutant embryos have central NS defects and holes

387   in the cuticle (Fig. 3A-F, supplementary Figs. 2 and 3A-F). As aqz^{GFP} behaves genetically as a

388   loss-of-function allele (does not complement all the deficiencies uncovering the locus tested with

389   similar phenotypes and theoretically all Aqz protein isoforms are affected), we mainly focused

390   our studies on aqz^{GFP}.

391

392   We used a genomic construct encompassing the aqz locus, and performed rescue experiments for

393   aqz^{GFP} and aqz^1 (Fig. 1A, Fig. 3G-J and supplementary Fig. 3G-I). Rescue experiments show

394   that aqz^{GFP} behaves as a loss-of-function allele, as a significant proportion of mutant embryos

395   survive embryogenesis and larval stages, and go on to emerge as viable adults (fertile males and

396   unfertile females) using one copy of the rescue construct (Fig. 3H-J). All the foregoing data,

397   taken as a whole and in conjunction with published data, establishes the CG9821 transcription

398   unit as being the aqz locus.

399

Gain of function phenotypes

401   Having two copies of the rescue construct did not increase embryonic rescue; rather, it proved

402   deleterious for larvae, as many died as larvae, and, as a consequence, significantly fewer reach

403   pupation, and adulthood (Fig. 3H). Two copies of the rescue construct in a wild type background

404   yielded a fraction of embryos with neurogenic defects (Fig. 3G), showing that loss and gain of

405   function conditions give similar results. These results suggest that Aqz isoforms abundance and

406   proportions are critical for normal development. Consistently, aqz^1 mutants show no adult

407   rescue; rather, if done with one or two rescue constructs, results show a significant increment in

408   the frequency of mutant phenotypes. This is consistent with at least a partial gain-of-function

409   nature for aqz^1, as the small Aqz protein is still present in aqz^1 (supplementary Fig. 3G-H).

410   Together with the rescue results of aqz^{GFP} and overexpression, this leads support to the notion

411   that the ratio and abundance of different Aqz protein isoforms is critical. We focused our studies

412   on the embryonic stages, where defects are first observed.

413

414 ***aqz* embryonic expression**

415 *aqz* embryonic expression is dynamic (Fig. 4). Expression is largely coincidental using a 5' *in*

416 *situ* probe from the locus, the *aqz*^GFP GFP expression in heterozygotes, and the anti-Aqz

417 antibody, meaning that transcription and translation are not differentially regulated. This

418 coincidental expression of GFP::Aqz with the anti-Aqz antibody staining in *aqz*^GFP heterozygotes

419 can be used as a marker for Aqz expression (Fig. 4). *aqz*^GFP homozygotes have a clumped,

420 abnormal accumulation of GFP::Aqz, in many cases appearing nuclear. This altered expression

421 serves as a marker for homozygous mutant embryos (for example, see Fig. 6G). During early

422 embryogenesis in the syncytial blastoderm (Fig. 4, st. 5), expression is seen in the peripheral

423 cytoplasm and centrally located nuclei of future vitellophages. In later stages, during germband

424 extension/retraction and dorsal closure stages, the ectoderm is heavily labeled, particularly the

425 neuroectoderm. There is also mesodermal Aqz labeling (Fig. 4, st. 9-10 and 14). During

426 germband retraction, the peripheral nervous system (PNS) and ectoderm are labeled, and some

427 amnioserosa cells nuclei (Fig. 4, st. 14). As the NS condenses and embryogenesis finishes, the

428 NS expresses *aqz* again, whereas the epidermal tissue expression diminishes (Fig. 4, st. 17). This

429 expression pattern is consistent with *aqz* requirements in ectoderm and ectodermally derived

430 embryonic tissues.

431

432 ***aqz* ectodermally-derived mutant phenotypes**

433 Two previous genetic screens identified *aqz* during embryogenesis. Mutant *aqz* germline clones

434 generated dead embryos with anterior and dorsal holes (Perrimon et al., 1996). RNAi injection in

435 developing wild type embryos lead to underdeveloped commissures in the ventral nerve cord,

436 resulting in widening of the distance between longitudinal connectives of the ventral nerve cord

437 commissures (VNC), and severe hypoplasia of the PNS (Ivanov et al., 2004). In both cases, end-

438 of-embryogenesis phenotypes were evaluated and not quantitated. Despite possible caveats (e.g.,

439 multiple mutant hits on the chromosome arm homozygosed for germline clones generation, and

440 putative specificity problems of RNAi, etc.) mutant phenotypes strongly implied multiple *aqz*

441 requirements in embryonic ectodermally derived tissues.

442

443 We used 22C10 and BP102 antibodies to examine nervous system commissures and the PNS,

444 and anti-Elav plus anti-coracle antibodies to examine post mitotic neurons and epidermis,

445   respectively. In late stage wild type embryos, there is co-expression of Coracle and Aqz proteins

446   in the epidermis, especially in the anterior compartment of every segment (Fig. 5A). In contrast,

447   there is no overlap with Elav staining (Fig. 5B), but there is a clear overlap in some somas of the

448   PNS throughout the body (Fig. 5C). Finally, there is no overlap with Repo protein in glial cells

449   (Fig. 5D). We examined embryonic defects in *aqz^{GFP}*, *aqz^1*, and other *aqz* mutant alleles. We

450   wanted to know whether results reported for embryonic RNAi injections and germline clones

451   would be similar. We corroborated and extended the *aqz* mutant cuticles and the disarray of the

452   NS findings reported previously (Ivanov et al., 2004; Perrimon et al., 1996). We first quantified

453   the number of *aqz^{GFP}* mutant homozygotes that die during embryogenesis. We separated and

454   cultured homozygous mutant *aqz^{GFP}* embryos alongside wild type Oregon R control embryos,

455   and found that 65.5% (n=417) die as embryos, before hatching, whereas only 20.8% Oregon R

456   embryos fail to hatch (n=173). All *aqz^{GFP}* mutant larvae fail to reach adulthood. A percentage of

457   *aqz^{GFP}* mutant embryos exhibit lack of or abnormal commissures and a strong reduction of the

458   PNS, and sport dorsal, lateral and/or ventral holes in the cuticle (Fig. 3A-F). *aqz^1* mutant

459   embryos show the same phenotypes (supplementary Fig. 3A-F). All other alleles examined

460   showed similar mutant phenotypes (supplementary Fig. 2). Mutant embryos also exhibit

461   neurogenic-like phenotypes and cell polarity defects, consistent with Aqz being required in the

462   developing ectoderm (see below).

463

464   Our expression results, the germline clones, and the RNAseq data from modEncode all suggest

465   an *aqz* maternal contribution partly fulfilling early Aqz requirements. These data firmly establish

466   an *aqz* requirement for ectoderm development and differentiation. Since these are the first *aqz*

467   mutant phenotypes, we focused on these embryonic ectodermal phenotypes, as they may help

468   explain later ones.

469

470   ***aqz* NS phenotypes**

471   We wanted to study when are NS defects first seen in *aqz* mutants. To study this, we stained

472   mutant embryos at different stages with different markers of the differentiating NS (Fig. 6). *aqz^1*

473   mutant embryos does not seem to have a different number of Achaete-positive staining cells

474   (Fig. 6A compared to 6B). Later, during germband extension/retraction, *aqz^1* mutant embryos

475   have a non-significant, but higher number of Deadpan-staining cells, that labels delaminating

476 neuroblasts (Fig. 6C compared to 6D). *aqz^1* heterozygotes have 121 $\pm$ 15.4 Deadpan-positive

477 cells per embryo (n=12), while *aqz^1* mutant homozygotes have 157 $\pm$ 22.Deadpan–positive cells

478 per embryos (n=16). *aqz^GFP* mutant embryos, also stained with Deadpan antibodies, show

479 irregular staining. Some embryonic areas show increased density of Deadpan positive cells,

480 whereas other areas show a dearth of labeled cells (Fig. 6I compared to 6J). Cells are irregularly

481 spaced, with some areas of the embryo showing ectopic stained cells (Fig. 6I, 6I compared to 6K,

482 6L). In a complementary fashion, in the mutant, clumped Aqz protein accumulation (in this

483 instance the chimeric GFP::Aqz) occurs where there is little or no Deadpan staining (Fig. 6G

484 compared to 6H). A similar phenotype is seen in *aqz^1*: Deadpan positive cells are irregularly

485 spaced (compare Fig. 6C with 6D). Aqz expression increases early before neuroblast

486 delamination, and decreases after the neuroblasts have delaminated, and start dividing (Fig. 4). In

487 *aqz^1*, ganglion mother cells are much reduced and irregularly spaced, as labeled by Anti-Eve

488 antibodies (Fig. 6E compared to 6F). This may mean that some mutant neuroblasts fail to

489 properly differentiate to ganglion mother cells, or differentiate later, a rationale that may explain

490 the tendency of an increased number of neuroblasts.

491

492 By stage 16, Aqz is expressed in the epidermis (Fig. 5A). Using epidermal markers, some parts

493 of the ectoderm show lack of staining (Fig. 7A-I). In these areas, there are more Deadpan-

494 positive cells, suggesting ectopic neuroblasts have formed at the expense of epidermal precursors

495 (Fig. 7A-I compared to O-S). This could explain the lack of cuticle in some parts, and as a

496 consequence, the cuticular holes found in dead embryos, strongly suggesting a neurogenic

497 phenotype.

498

499 Aqz, Notch pathway and epithelial polarity

500 The Notch pathway regulates neuroblast and epidermoblast numbers and specification via lateral

501 inhibition during ectoderm differentiation (Campos-Ortega and Knust, 1990; Hartenstein et al.,

502 1992). *Aqz* mutants show perturbed neurogenesis and epidermogenesis, with phenotypes akin to

503 Notch mutants, i.e. neurogenic phenotypes.

504

505 How can Aqz affect Notch signaling? One possibility is that Aqz alters epithelial cell polarity,

506 which is known to affect the apical localization of Dl and consequently, its interaction with the

507   Notch receptor (Krahn and Wodarz, 2009). In order to study epithelial polarity, we used

508   antibodies against different known epithelial polarity markers in aqz^{GFP} embryos. We used anti-

509   Crumbs antibodies (anti-Crb) as an apical domain marker (fig. 8 A-H), and anti-Discs large

510   antibodies (anti-Dlg) as a basolateral marker (Fig. 8I-P). Results show that the apical domain is

511   compromised, showing reduced Crumbs staining, whereas the basolateral domain is expanded

512   (Discs large staining is augmented).

513

514   We then asked whether adherens junctions and Delta expression are altered. We used DE-

515   cadherin antibodies as an adherens junction marker. Adherens junctions are also compromised,

516   since DE-cadherin shows significantly reduced and patchy staining in aqz^{GFP} homozygotes, and

517   so does Dl expression, which is also reduced and patchy (Fig. 8Q,-X).

518

519   Altogether, the altered epithelial polarity and consequent reduced Dl expression, may explain the

520   neurogenic phenotypes associated with aqz mutants, and the ectodermally derived aqz

521   phenotypes. This implies cell polarization defects starting at neurulation being the ultimate cause

522   of aqz mutant defects and lethality, and provide an explanation for aqz involvement in

523   ectodermally derived tissues. It would be interesting to investigate whether other epithelia at

524   other stages also bear similar defects.

525

526   **Discussion**

527   *aaquetzalli* is a complex locus encompassing at least three different mRNAs and three different

528   protein products. They code for proteins with a conserved domain, the PNRC, of which *D.*

529   *melanogaster* harbors two genes. Vertebrate genes with such a domain function in nonsense-

530   mediated RNA decay proteins, and interact with nuclear receptors of varied function. What does

531   Aqz do? Having a second gene with the same conserved domain might mean they are redundant,

532   or partially redundant, and that some functions might be masqued by the activity of the other,

533   even if they diverged somewhat and acquired new functions. Coding for multiple proteins also

534   means that unless we mutate all forms (like in aqz^{GFP}), we might not get a 'pure' loss-of-function

535   phenotype, and instead have complicated alleles that may be at the same time loss and gain of

536   function. It also leads to complex complementation patterns and phenotypes. Regardless, we

537   observe that most of the phenotypes are consistent, and, in embryos, affect the ectoderm and

538 ectodermally derived tissues.

539

540 Why is the phenotype partial in embryos? We know penetrance is not 100% (not all mutant

541 embryos die). We reason that besides the second PNRC-containing gene alluded to above, there

542 is maternal contribution, that may obscure early mutant phenotypes. In aqz^{GFP} adults are never

543 seen, with death occurring during a prolonged phenocritical period from embryogenesis to

544 pupariation. From this, we sought to study the earliest defects, in order to gain insight into the

545 causes originating the mutant phenotypes. We found that these phenotypes start very early,

546 around cellularization and cell polarization.

547

548 We also show here that Aqz is expressed throughout the life cycle, and is pleiotropic. Yet we

549 find it works in cell polarity early in development, setting the stage for organ differentiation in

550 ectodermally derived tissues, like the epidermis and the NS. We also show that the common

551 thread for these defects is cell polarization, in particular, loss or reduction of the apical domain.

552 This in turn, leads to compromised Dl and adherens junctions (AJ) localization and abundance

553 (evidenced by Dl and E-Cad staining, respectively), and a neurogenic-like phenotype.

554

555 Other genes, besides Notch genes, have neurogenic phenotypes. Some have cell polarity defects,

556 like the cell polarity regulatory proteins (CPRPs), that promote distribution of cellular

557 components (i.e., E-cadherin, a component of AJ, and Dl) in asymmetric patterns resulting in

558 polarized cells (Sasaki et al., 2007). Abnormal conditions in these genes, by way of cell polarity

559 defects, may lead to the defects seen in aqz mutants. The way in which they cause these defects

560 is currently unknown, but would be interesting to see whether they interact with Aqz in flies, or

561 an Aqz-like vertebrate protein, as Aqz behaves much like them.

562

563 **Conclusions**

564 In this paper we have studied the embryonic epithelial defects of aqz mutants, specially in the

565 embryonic ectoderm, and ectodermally derived tissues. We have found that there is a defective

566 neural / epithelial development and differentiation, and that these defects could be ascribed to

567 faulty epithelial polarization. It remains to be seen whether aqz, being transcribed at all stages of

568 the life cycle, is similarly required for other epithelial polarization processes, like in the

569   compound eye or in the wing epithelia. It also remains to be seen whether the *aqz* maternal

570   contribution is requied earlier in development, and whether the other PNRC-domain-containing

571   protein in the fly genome indeed is partially redundant with Aqz function.

572

Acknowledgements

574   We acknowledge assistance of Peña-Rangel.

575

576

References

578

579   Bayraktar, J., Zygmunt, D. and Carthew, R.W., 2006. Par-1 kinase establishes cell polarity and
580   functions in Notch signaling in the Drosophila embryo. J Cell Sci. 119, 711-21.
581   Bertrand, N., Castro, D.S. and Guillemot, F., 2002. Proneural genes and the specification of
582   neural cell types. Nat Rev Neurosci. 3, 517-30.
583   Buszczak, M., Paterno, S., Lighthouse, D., Bachman, J., Planck, J., Owen, S., Skora, A.D.,
584   Nystul, T.G., Ohlstein, B., Allen, A., Wilhelm, J.E., Murphy, T.D., Levis, R.W., Matunis,
585   E., Srivali, N., Hoskins, R.A. and Spradling, A.C., 2007. The carnegie protein trap
586   library: a versatile tool for Drosophila developmental studies. Genetics. 175, 1505-31.
587   Cabrera, C.V., 1990. Lateral inhibition and cell fate during neurogenesis in Drosophila: the
588   interactions between scute, Notch and Delta. Development. 110, 733-42.
589   Campos-Ortega, J.A. and Hartenstein, V., 1997. The embryonic development of Drosophila
590   melanogaster, 2nd ed. Springer, Berlin ; New York.
591   Campos-Ortega, J.A. and Knust, E., 1990. Molecular analysis of a cellular decision during
592   embryonic development of Drosophila melanogaster: epidermogenesis or neurogenesis.
593   Eur J Biochem. 190, 1-10.
594   Celniker, S.E., Dillon, L.A., Gerstein, M.B., Gunsalus, K.C., Henikoff, S., Karpen, G.H., Kellis,
595   M., Lai, E.C., Lieb, J.D., MacAlpine, D.M., Micklem, G., Piano, F., Snyder, M., Stein,
596   L., White, K.P., Waterston, R.H. and mod, E.C., 2009. Unlocking the secrets of the
597   genome, Nature. pp. 927-30.
598   Cornell, R.A. and Ohlen, T.V., 2000. Vnd/nkx, ind/gsh, and msh/msx: conserved regulators of
599   dorsoventral neural patterning? Curr Opin Neurobiol. 10, 63-71.
600   Dos Santos, G., Schroeder, A.J., Goodman, J.L., Strelets, V.B., Crosby, M.A., Thurmond, J.,
601   Emmert, D.B., Gelbart, W.M. and FlyBase, C., 2015. FlyBase: introduction of the
602   Drosophila melanogaster Release 6 reference genome assembly and large-scale migration
603   of genome annotations. Nucleic Acids Res. 43, D690-7.
604   Dunn, J.G., Foo, C.K., Belletier, N.G., Gavis, E.R. and Weissman, J.S., 2013. Ribosome
605   profiling reveals pervasive and regulated stop codon readthrough in Drosophila
606   melanogaster. Elife. 2, e01179.
607   Edgar, R., Domrachev, M. and Lash, A.E., 2002. Gene Expression Omnibus: NCBI gene
608   expression and hybridization array data repository. Nucleic Acids Res. 30, 207-10.
609   Egger, B., Chell, J.M. and Brand, A.H., 2008. Insights into neural stem cell biology from flies.
610   Philos Trans R Soc Lond B Biol Sci. 363, 39-56.

611   Fehon, R.G., Johansen, K., Rebay, I. and Artavanis-Tsakonas, S., 1991. Complex cellular and
612   subcellular regulation of notch expression during embryonic and imaginal development
613   of Drosophila: implications for notch function. J Cell Biol. 113, 657-69.

614   Feinberg, A.P. and Vogelstein, B., 1984. A technique for radiolabeling DNA restriction

615   endonuclease fragments to high specific activity. Anal Biochem. 137, 266-7.

616   Fortini, M.E., 2009. Notch signaling: the core pathway and its posttranslational regulation. Dev
617   Cell. 16, 633-47.
618   Fortini, M.E. and Artavanis-Tsakonas, S., 1993. Notch: neurogenesis is only part of the picture.
619   Cell. 75, 1245-7.
620   Harris, K.P. and Tepass, U., 2008. Cdc42 and Par proteins stabilize dynamic adherens junctions
621   in the Drosophila neuroectoderm through regulation of apical endocytosis. J Cell Biol.
622   183, 1129-43.
623   Harris, K.P. and Tepass, U., 2010. Cdc42 and vesicle trafficking in polarized cells. Traffic. 11,
624   1272-9.
625   Harris, T.J., 2012. An introduction to adherens junctions: from molecular mechanisms to tissue
626   development and disease. Subcell Biochem. 60, 1-5.
627   Hartenstein, A.Y., Rugendorff, A., Tepass, U. and Hartenstein, V., 1992. The function of the
628   neurogenic genes during epithelial development in the Drosophila embryo. Development.
629   116, 1203-20.
630   Hartenstein, V. and Wodarz, A., 2013. Initial neurogenesis in Drosophila. WIREs Dev Biol.
631   Ivanov, A.I., Rovescalli, A.C., Pozzi, P., Yoo, S., Mozer, B., Li, H.P., Yu, S.H., Higashida, H.,
632   Guo, V., Spencer, M. and Nirenberg, M., 2004. Genes required for Drosophila nervous
633   system development identified by RNA interference. Proc Natl Acad Sci U S A. 101,
634   16216-21.
635   Jagadeeshan, S. and Singh, R.S., 2005. Rapidly evolving genes of Drosophila: differing levels of
636   selective pressure in testis, ovary, and head tissues between sibling species. Mol Biol
637   Evol. 22, 1793-801.
638   Karcavich, R.E., 2005. Generating neuronal diversity in the Drosophila central nervous system: a
639   view from the ganglion mother cells. Dev Dyn. 232, 609-16.
640   Karr, T.L. and Alberts, B.M., 1986. Organization of the cytoskeleton in early Drosophila
641   embryos. J Cell Biol. 102, 1494-509.
642   Kelso, R.J., Buszczak, M., Quinones, A.T., Castiblanco, C., Mazzalupo, S. and Cooley, L., 2004.
643   Flytrap, a database documenting a GFP protein-trap insertion screen in Drosophila
644   melanogaster. Nucleic Acids Res. 32, D418-20.
645   Kooh, P.J., Fehon, R.G. and Muskavitch, M.A., 1993. Implications of dynamic patterns of Delta
646   and Notch expression for cellular interactions during Drosophila development.
647   Development. 117, 493-507.
648   Krahn, M.P. and Wodarz, A., 2009. Notch signaling: linking delta endocytosis and cell polarity.
649   Dev Cell. 17, 153-4.
650   Lai, T., Cho, H., Liu, Z., Bowler, M.W., Piao, S., Parker, R., Kim, Y.K. and Song, H., 2012.
651   Structural basis of the PNRC2-mediated link between mrna surveillance and decapping.
652   Structure. 20, 2025-37.
653   Liu, S., Bonner, J.M., Chanet, S., Commisso, C., Skwarek, L.C., Schweisguth, F. and Boulianne,
654   G.L., 2012. Functional analysis of the NHR2 domain indicates that oligomerization of

655   Neuralized regulates ubiquitination and endocytosis of Delta during Notch signaling. Mol
656   Cell Biol. 32, 4933-45.
657 Nicol, J.W., Helt, G.A., Blanchard, S.G., Jr., Raja, A. and Loraine, A.E., 2009. The Integrated
658   Genome Browser: free software for distribution and exploration of genome-scale
659   datasets. Bioinformatics. 25, 2730-1.
660 Nusslein-Volhard, C. and Wieschaus, E., 1980. Mutations affecting segment number and polarity
661   in Drosophila. Nature. 287, 795-801.
662 Pai, L.M., Kirkpatrick, C., Blanton, J., Oda, H., Takeichi, M. and Peifer, M., 1996. Drosophila
663   alpha-catenin and E-cadherin bind to distinct regions of Drosophila Armadillo. J Biol
664   Chem. 271, 32411-20.
665 Peifer, M. and Wieschaus, E., 1990. The segment polarity gene armadillo encodes a functionally
666   modular protein that is the Drosophila homolog of human plakoglobin. Cell. 63, 1167-76.
667 Perrimon, N., Lanjuin, A., Arnold, C. and Noll, E., 1996. Zygotic lethal mutations with maternal
668   effect phenotypes in Drosophila melanogaster. II. Loci on the second and third
669   chromosomes identified by P-element-induced mutations. Genetics. 144, 1681-92.
670 Portin, P., 2002. General outlines of the molecular genetics of the Notch signalling pathway in
671   Drosophila melanogaster: a review. Hereditas. 136, 89-96.
672 Sambrook, J., Fritsch, E.F. and Maniatis, T., 1989. Molecular Cloning: A Laboratory Manual,
673   2nd edition ed. Cold Spring Harbor Laboratory Press, New York.
674 Sasaki, N., Sasamura, T., Ishikawa, H.O., Kanai, M., Ueda, R., Saigo, K., Matsuno, K., 2007.
675   Polarized exocytosis and transcytosis of Notch during its apical localization in
676   Drosophila epithelial cells. Genes Cells 12(1): 89--103.
677 Schrons, H., Knust, E. and Campos-Ortega, J.A., 1992. The Enhancer of split complex and
678   adjacent genes in the 96F region of Drosophila melanogaster are required for segregation
679   of neural and epidermal progenitor cells. Genetics. 132, 481-503.
680 Skeath, J.B., Panganiban, G., Selegue, J. and Carroll, S.B., 1992. Gene regulation in two
681   dimensions: the proneural achaete and scute genes are controlled by combinations of
682   axis-patterning genes through a common intergenic control region. Genes Dev. 6, 2606-
683   19.
684 St Pierre, S.E., Ponting, L., Stefancsik, R., McQuilton, P. and FlyBase, C., 2014. FlyBase 102--
685   advanced approaches to interrogating FlyBase. Nucleic Acids Res. 42, D780-8.
686 Stapleton, M., Carlson, J., Brokstein, P., Yu, C., Champe, M., George, R., Guarin, H.,
687   Kronmiller, B., Pacleb, J., Park, S., Wan, K., Rubin, G.M. and Celniker, S.E., 2002. A
688   Drosophila full-length cDNA resource. Genome Biol. 3, RESEARCH0080.
689 Tautz, D. and Pfeifle, C., 1989. A non-radioactive in situ hybridization method for the
690   localization of specific RNAs in Drosophila embryos reveals translational control of the
691   segmentation gene hunchback. Chromosoma. 98, 81-5.
692 Technau, G.M., Berger, C. and Urbach, R., 2006. Generation of cell diversity and segmental
693   pattern in the embryonic central nervous system of Drosophila. Dev Dyn. 235, 861-9.
694 Tepass, U., 2012. The apical polarity protein network in Drosophila epithelial cells: regulation of
695   polarity, junctions, morphogenesis, cell growth, and survival. Annu Rev Cell Dev Biol.
696   28, 655-85.
697 Tepass, U., Gruszynski-DeFeo, E., Haag, T.A., Omatyar, L., Torok, T. and Hartenstein, V.,
698   1996. shotgun encodes Drosophila E-cadherin and is preferentially required during cell
699   rearrangement in the neurectoderm and other morphogenetically active epithelia. Genes
700   Dev. 10, 672-85.

701 Tian, L., Chen, J., Chen, M., Gui, C., Zhong, C. Q., Hong, L., Xie, C., Wu, X., Yang, L. , Ahmad V.,
702 and Han, J., 2014. The p38 pathway regulates oxidative stress tolerance by
703 phosphorylation of mitochondrial protein IscU. J Biol Chem 289 (46), 31856-31865.
704 Venken, K. J., Carlson, J. W., Schulze, K. L., Pan, H., He, Y., Spokony, R., Wan, K. H., Koriabine,
705 M., de Jong, P. J., White, K. P., Bellen, H. J., and Hoskins, R. A., 2009. Versatile
706 P[acman]
707 BAC libraries for transgenesis studies in Drosophila melanogaster." Nat Methods
708 **6**(6): 431-434.Wang, F., Dumstrei, K., Haag, T. and Hartenstein, V., 2004. The role of DE-
709 cadherin during cellularization, germ layer formation and early neurogenesis in the
710 Drosophila embryo. Dev Biol. 270, 350-63.
711 Weinmaster, G. and Fischer, J.A., 2011. Notch ligand ubiquitylation: what is it good for? Dev
712 Cell. 21, 134-44.
713 Wodarz, A., 2008. Extraction and immunoblotting of proteins from embryos. Methods Mol Biol.
714 420, 335-45.
715 Zhao, G., Wheeler, S.R. and Skeath, J.B., 2007. Genetic control of dorsoventral patterning and
716 neuroblast specification in the Drosophila Central Nervous System. Int J Dev Biol. 51,
717 107-15.
718 Zhong, W. and Chia, W., 2008. Neurogenesis and asymmetric cell division. Curr Opin
719 Neurobiol. 18, 4-11.
720 Zhou, D., Shen, R., Ye, J.J., Li, Y., Tsark, W., Isbell, D., Tso, P. and Chen, S., 2008. Nuclear
721 receptor coactivator PNRC2 regulates energy expenditure and adiposity. J Biol Chem.
722 283, 541-53.
723

724 **Figure Legends**

725

726 Figure 1. **The *aaquetzalli* (*aqz*) locus codes for at least three alternatively spliced transcripts.**

727 (A) *aqz* encompasses a little above 7 Kb, from 4647000 to 4638000 at the base of chromosome

728 3R at 85B2; in the figure the genes are oriented such that the 5' end of *aqz* is to the left. Besides

729 *aqz* (solid black arrow), other genes mapping in the region are shown as grey-hashed arrows. *aqz*

730 codes for four predicted different mRNA species, each with two exons (grey boxes) and one

731 intron (black line). Several cDNAs and ESTs (white boxes with black borders, and white boxes

732 with black dotted lines, respectively) map in the locus. Underneath the depicted chromosome

733 line a grey bar signals the extent of the genomic rescue construct employed (BAC CH322-

734 25015), inserted in the second chromosome at 53B2 (Bloomington line #9736). The location of

735 two transposon insertion mutants, one in the promoter region (*aqz²*), and one in the intron

736 (*aqz^{GFP}*), are shown. *aqz^{GFP}* is a fly trap line (#CB03335), coding for a predicted fusion protein,

737 where the GFP moiety is fused to the 5' end of Aqz. *aqz¹* has a four base pairs insertion,

738 depicted in bold, in the promoter region of *aqz* between the predicted TATA box and initiation of

739   transcription. aqz^1 was isolated as an imprecise excision of the aqz^2 transposon. Nearly all

740   isolated aqz alleles are lethal. (B) Aqz has a conserved domain at the 5' end of the protein. The

741   homology is for a proline-rich conserved domain of nuclear receptor co-activators (PNRC-

742   domain proteins) in single letter amino acid code, present in both invertebrate and vertebrate

743   proteins. Numbers to the left indicate position of the domain within the proteins. (C) Northern

744   blot using two different aqz cDNAs as probes reveal three different transcripts of 7.53, 5.03 and

745   3.16 Kb. The smallest band (3.16 Kb) is only present in adult flies, and is only seen using a 5'

746   cDNA (LD47990), present in all aqz isoforms. The same blot that was used with the first probe,

747   was photographed, then stripped, and re-probed with the a more 3' cDNA (LD02060), that

748   recognizes aqz RB, RC, and RD, but not aqz RA. n>10. (D) Aqz mutant and control Western

749   blot using an antibody against GFP recognizes a band at approximately 40 kD (right black

750   arrow) in aqz^{GFP} homozygotes, and weakly, in aqz^{GFP} heterozygotes. All other weak bands are

751   present in all lanes, including the control, wild type lane, and are, consequently, not specific.

752

753   Figure 2. ***aqz* has alterative splicing.** aqz mRNAs first exon is translated, and some have also 3'

754   stop codon read-through in the second exon, judging from ribosome footprinting data. The aqz

755   locus (CG9821) together with the annotated predicted mRNAs are depicted on top (green) with

756   dotted lines depicting introns, and red lines depicting other transcripts. The neighboring CG9837

757   locus, overlapping CG9821 at the 5' end, is also depicted in green. The ribosome footprinting

758   data is depicted below taken from S2 cells (black), 0-2 hrs. embryos (blue) and mRNA-seq

759   (gray) in reads per million. Inset shows a magnification of the Aqz C-terminal region where

760   protein extension may occur.

761

762   Figure 3. ***aqz^{GFP}* mutant phenotypes.** (A) and (B) show mutant (aqz^{GFP}/aqz^{GFP}) and wild type

763   cuticles, respectively, the former one with an anterior hole and head involution defects (white

764   arrow). (C) and (E) show mutant embryos stained with neuronal and epithelial markers: in (C)

765   anti-Elav for neuronal bodies and anti-Coracle (Cora) for epithelial cells, while in (E) 22C10 for

766   axons and some neuronal bodies. (D) and (F) show the same stainings using wild type control

767   embryos. Scale bar is 100 μm. (G) Shows the percentages of embryos with neural phenotypes in

768   aqz^{GFP}/aqz^{GFP} embryos, with one or two copies of a genomic rescue construct. One copy of the

769   rescue construct rescues significantly the mutant phenotype, whereas two copies effects a

770 significant, but smaller, rescue, pointing to some gain-of-function effects with two rescue
771 constructs. Two copies of the rescue construct in a wild type background have neurogenic
772 phenotypes in over 40% of embryos, phenotypes similar to *aqz* mutants. In (G) and (H) *aqz*^{GFP} is
773 homozygous mutant, *aqz*$^{RECUE/+}$ is one copy of the rescue construct, and *aqz*^{recue} indicates two
774 copies of the rescue construct. (H) Extended phenocritical period of *aqz*^{GFP}/*aqz*^{GFP}mutants. The
775 surviving *aqz*^{GFP}/*aqz*^{GFP} mutant embryos die majorly as larvae, with approximately 20%
776 reaching pupariation. No adults are ever observed. The *aqz*^{GFP}/*aqz*^{GFP} lethality is rescued to wild
777 type levels with one copy of the *aqz* genomic rescue construct, but two copies of the rescue
778 construct, while having a significant rescue effect, are less effective, pointing to some gain-of-
779 function effects with two rescue constructs. (I) *aqz*^{GFP}/*aqz*^{GFP} mutant pupae die early, with
780 necrosis (left side pupae, black arrow), compared to a control pupae (right side pupae). Scale bar
781 is 1mm. (J) Rescued *aqz*^{GFP}/*aqz*^{GFP} mutant fly (top) compared to sibling control fly (bottom, has
782 curved wings as marker). In this and all figures, ** denotes significant differences. In all figures,
783 for all embryo experiments, representative ones are shown, and n examined is over 200 per
784 condition.

785

786 Figure 4. **Aqz mRNAs and proteins are expressed throughout embryogenesis in the**
787 **ectoderm and in ectodermally derived structures, and have maternal contribution.** (A)
788 Anti-sense *aqz in situ* hybridization results at different embryonic stages of development; (B)
789 shows results with the sense control probe (both derived from *aqz* cDNA LD47990). Embryos in
790 (C) are stained with the anti-Aqz antibody, (1:100), whereas (D) shows expression of chimeric
791 GFP::Aqz proteins using an anti GFP antibody (1:100) from the same embryos, which are
792 heterozygous for *aqz*^{GFP}, and thus, have expression of both GFP::Aqz and native Aqz protein.
793 As shown in (E), results from both are largely coincidental except some PNS cells and some
794 amnioserosa cells, only labeled with the anti-Aqz antibody. In all panels, anterior is left and
795 dorsal is up. All views are lateral views except the lower row, where ventrolateral views are
796 shown to evidence the developing central nervous system. Stage 5 early syncytial embryo, stage
797 9-10 germband extension/retraction stages, stage 14 dorsal closure, and stage 17, end of
798 embryogenesis. Scale bar is 100 μm.

799

800   Figure 5. **Aqz expressed in ectodermally derived tissue.** Panel (A) shows an anti-GFP staining

801   for GFP::Aqz expression together with an epidermal marker, anti-Cora, showing some

802   coincidental expression (yellow). For all immune-stainings in the figure, the panels marked

803   underneath the top panels A-D labeled E-F show the GFP::Aqz channel separate, and the panels

804   G-H show the anti-Aqz. The bottom row of panels marked with I, J, K and L depict the anti-

805   coracle (I), anti-Elav (J), anti-22C10 (K), and anti-repo (L) channels, respectively. Panel (B)

806   shows anti-GFP for GFP::Aqz and anti-Elav, to mark neuronal cells in the developing central

807   NS. (C) Using monoclonal 22C10, there is coincidental expression with anti-Aqz antibody,

808   showing that some neurons in the PNS are positive for both Aqz and 22C10 (yellow). (D) In

809   contrast no glial cells (marked by anti-Repo antibody) are coincidental with anti-Aqz antibody

810   staining, showing that glial cells do not express Aqz. Scale bar is 100 µm.

811

812   Figure 6. *aqz* **NS defects are detected from the onset of NS formation.** (A, C, E and G) are *aqz*

813   homozygous mutant embryos stained with markers for the NS. (B, D, F and H) are

814   corresponding heterozygous embryos (controls). All views are lateral with anterior to the left,

815   dorsal up. A and B show anti-Achaete staining marking proneural cell during germband

816   extension/retration. C and D show deadpan marked neuroblasts during germband

817   extension/retration and condensation of the NS. Notice irregular appearance of neuroblasts in C

818   compared with D (control). E and F show expression of Evenskipped (Eve), marking ganglion

819   mother cells, showing a disruption in the mutant (compare E to F) at this later stage of

820   development (stage 15). G and H mark expression of GFP::Aqz. Green lines underneath G mark

821   parts of the embryo with abnormal GFP::Aqz expression, compared to H, where the GFP::Aqz

822   signal is distributed homogeneously. I marks neuroblasts. They also show a clumped and

823   irregular distribution (compare to J which shows a regular array of neuroblasts). Red lines mark

824   areas with abundant neuroblasts in I. K and L show the merged images. Scale bar is 100 µm.

825

826   Figure 7. **Mutations in Aqz lead to irregular distribution of epithelial tissue and NS.** A and

827   O show lateral views of embryos (anterior to the left and dorsal up) stained for neuroblasts

828   (Deadpan antibodies, red), epithelia (Coracle antibodies, yellow), also showing expression of

829   Aqz (green). Scale bar is 100 µm. In A, two distinct regions showing irregular distribution of

830   labels: A1 and A2, are enclosed in white rectangles and enlarged to the right. For comparison, a

831   similar control area is shown in O, the heterozygous control embryo. B', F and P show enlarged

832   anti-Deadpan staining (red); C, G and Q show enlarged GFP::Aqz expression, D, H and R show

833   enlarged anti-Coracle expression, whilst E, I and S show merged images, respectively. Scale bar

834   is 50 µm. J-N show another example of lack of epithelial cells using a different epidermal marker

835   (anti-FasIII, K) and an irregular distribution of neuroblasts (anti-Deadpan, L) in aqz^{GFP} mutant

836   embryos (GFP::Aqz, J). Nuclei are labeled by DAPI (M). N show the respective merged image.

837

838   Figure 8. **The *aqz* mutant neuroepthelium has polarity defects.** A, E, I, M, Q, and U are lateral

839   views of embryos undergoing dorsal closure, with anterior to the left and dorsal up. Bars are 100

840   µm. A-D, I-L, and Q-T are aqz^{GFP} mutant embryos, whereas E-H, M-P, and U-X are aqz^{GFP}

841   heterozygtes as controls. B, F, J, N, R, and V show GFP::Aqz expression, C and G anti-Crumbs

842   (Crb) (red), K and O anti-Discs large (Dlg) (red), and S and W anti-Delta (Dl) (yellow). D, H,

843   L, and P show respective merged images. Scale bar is 50 µm. T and X show anti-DE-cadherin

844   (DE-Cad) (red). Note that homozygous mutant GFP::Aqz expression appears more clumped

845   compared to the heterozygous controls, as stated before, and aids in identification of mutant

846   embryos.

847

848   Figure S1. *aqz* locus cDNAs partially sequenced. We sequenced both the 5' and 3' ends of

849   SD19655 and RE74095 to help us piece together the extent of the transcripts of the locus.

850

851   Figure S2. Other *aqz* mutant alleles have ectoderm-derived mutant phenotypes. (A) shows

852   cuticular phenotypes; mutant embryos have holes in various positions (dorsal, lateral, anterior),

853   compared to a wild type cuticle (bottom left). (B) shows nervous system staining using the Elav

854   staining, where clear deformities of the central nervous system are shown, compared to the wild

855   type (bottom panel). (C) shows anti-22C10 staining marking neuronal somas and the peripheral

856   nervous system. *aqz* mutant embryos have irregularities in the disposition of the peripheral

857   nervous system, as well as abnormal regions of low and high density of peripheral nervous

858   system cells, compared to wild type (bottom panel). (D) shows anti-BP102 staining showing

859   abnormalities in *aqz* mutant connectives in the ventral nervous chord in late embryos (wild type

860   control, bottom panel). All embryos are shown with anterior to the left and dorsal up.

861

862   Figure S3. *aqz¹* mutant phenotypes. (A) *aqz¹* mutants have a cuticular phenotype, similar to

863   *aqzᴳᶠᴾ*, but at a lower penetrance. *aqz¹* cuticles have holes (arrows), compared to (B), a wild type

864   cuticle. Mutant *aqz¹* embryos have nervous system phenotypes similar to *aqzᴳᶠᴾ* as (C) shows a

865   disorganized and deformed nervous system stained with anti-Elav (top panel), and also shows

866   abnormal epithelial tissue, as marked by anti-Coracle staining (middle panel). Lower panel

867   shows a merged image. (D) shows a similarly stained control embryo. (E) shows an *aqz¹* mutant

868   embryo displaying abnormal peripheral nervous system, as evidenced by anti-22C10 staining,

869   compared to (F), a wild type control embryo. In all panels, embryos are shown with dorsal up

870   and anterior left. Scale bar are 100 μm. (F) shows a quantification of *aqz¹* nervous system

871   phenotypes, akin to neurogenic phenotypes, in roughly a third of mutant embryos. Two copies of

872   a genomic rescue construct significantly increase this percentage: over 60% embryos with the

873   rescue constructs exhibit a neurogenic phenotype. (H) The majority of *aqz¹* embryos that survive

874   embryogenesis die as pupae, with a few (less than 10%) dying as larvae. Adding two *aqz*

875   genomic rescue constructs significantly increases the number of larvae (over 50%) that do not

876   reach pupation. In (G) and (H) adding wild type copies of *aqz* increases the *aqz¹* mutant

877   phenotypes, similar to the effect of two rescue wild type copies of *aqz* in *aqzᴳᶠᴾ* homozygotes.

878   (I) shows two *aqz¹* mutant pupae with necrotic patches (black arrows) (left and middle pupae),

879   compared to a wild type control pupa (right). Scale bar 1mm. Anterior is up.

880

881   Figure S4. *aqz¹* has mutant phenotypes in epidermis and nervous system. A and C show mutant

882   embryos, while B and D show similarly stained control embryos (heterozygotes). A and B show

883   anti-Deadpan for neuroblasts, and anti-Fascilin III to mark the epithelium. Note disorganization

884   in the mutant embryos. Scale bar is 100 μm. C and D show anti-BP102 staining, showing

885   abnormalities in mutant connectives in the ventral nervous chord. All embryos are oriented

886   dorsal up and anterior left.

887

888   Table 1. *aqz* alleles *c*omplementation matrix. *aqzⁱⁿˢᵉʳᵗⁱᵒⁿ* (*aqz²*) is homozygous viable and

889   complements *aqz¹*, which is homozygous lethal. *aqzᴳᶠᴾ* (another P-element insertion), is

890   homozygous lethal. *aqz¹* complements *aqzᴳᶠᴾ* and all three *aqz*-uncovering deficiencies

891   (*Df(3R)Exel6150, Df(3R)BSC478*, and *Df(3R)BSC506*). *aqzᴳᶠᴾ* does not complement these

892   deficiencies. + Indicates complementation, L indicates non-complementation (lethality), HV

893   indicates homozygous viable, and HL indicates homozygous lethal. *Df(3R)Exel6150* deletes

894   85A5-B6, *Df(3R)BSC478* deletes 85A5-B8, and *Df(3R)BSC506* deletes 85B1-C2. Together, the

895   common deleted fragment goes from 85B1-B6. The *aqz* locus is located at 85B2.

896

897   Table S1. *Df(3R)Exel6150* and *aqz^{GFP}* genetically complement stocks with insertions on *aqz*

898   neighboring genes. *Df(3R)Exel6150* and *aqz^{GFP}* are homozygous lethal, but fully complement

899   insertions in *CG9836*, *CR43130*, *CG9837* and *CG8359*. + indicates complementation and ND

900   indicates not determined. The crosses between *Df(3R)Exel6150* and mutant alleles

901   produced adults with and without balancers (for *P{EP}IscUG18758(CG9836)*= 70 with and

902   41 without balancers, for *P{SUPor-P}KG08159ry506(CR43130)*= 18 with and 82 without

903   balancers and for *Mi{MIC}CG9837MI01411(CG9837)*= 49 with and 81 without balancers). Also

904   the crosses between *aqz^{GFP}* and mutant alleles produced adults with and without balancers

905   (for *P{EP}IscUG18758(CG9836)*= 105 with and 77 without balancers, for *P{SUPor-*

906   *P}KG08159ry506(CR43130)*= 106 with and 64 without balancers, for

907   *Mi{MIC}CG9837MI01411(CG9837)*= 35 with and 53 without balancers and

908   *P{EPgy2}hng2EY18943(CG8359)*= 23 with and 50 without balancers).

909

aqz alleles complementation matrix.

aqz^insertion (*aqz²*) is homozygous viable and complements *aqz¹*, which is homozygous lethal. *aqz^GFP* (another P-element insertion), is homozygous lethal. *aqz¹* complements *aqz^GFP* and all three *aqz*-uncovering deficiencies (*Df(3R)Exel6150, Df(3R)BSC478*, and *Df(3R)BSC506*). *aqz^GFP* does not complement these deficiencies. + Indicates complementation, L indicates non-complementation (lethality), HV indicates homozygous viable, and HL indicates homozygous lethal. *Df(3R)Exel6150* deletes 85A5-B6, *Df(3R)BSC478* deletes 85A5-B8, and *Df(3R)BSC506* deletes 85B1-C2. Together, the common deleted fragment goes from 85B1-B6. The *aqz* locus is located at 85B2.

1 **Table 1**

Allele	aqz^1	aqz^2	aqz^{GFP}	Df(3R)Exel6150	Df(3R)BSC478	Df(3R)BSC506
aqz^1	HL	+	+	+	+	+
aqz^2		HV	+	+	+	+
aqz^{GFP}			HL	L	L	L
Df(3R)Exel6150				HL	L	L
Df(3R)BSC478					HL	L
Df(3R)BSC506						HL

3
4

Figure 1

The *aaquetzalli* (*aqz*) locus codes for at least three alternatively spliced transcripts

(A) *aqz* encompasses a little above 7 Kb, from 4647000 to 4638000 at the base of chromosome 3R at 85B2; in the figure the genes are oriented such that the 5' end of *aqz* is to the left. Besides *aqz* (solid black arrow), other genes mapping in the region are shown as grey-hashed arrows. *aqz* codes for four predicted different mRNA species, each with two exons (grey boxes) and one intron (black line). Several cDNAs and ESTs (white boxes with black borders, and white boxes with black dotted lines, respectively) map in the locus. Underneath the depicted chromosome line a grey bar signals the extent of the genomic rescue construct employed (BAC CH322-25015), inserted in the second chromosome at 53 B 2 (Bloomington line #9736). The location of two transposon insertion mutants, one in the promoter region (*aqz²*), and one in the intron (*aqz^{GFP}*), are shown. *aqz^{GFP}* is a fly trap line (#CB03335), coding for a predicted fusion protein, where the GFP moiety is fused to the 5' end of Aqz. *aqz¹* has a four base pairs insertion, depicted in bold, in the promoter region of *aqz* between the predicted TATA box and initiation of transcription. *aqz¹* was isolated as an imprecise excision of the *aqz²* transposon. Nearly all isolated *aqz* alleles are let h al. (B) Aqz has a conserved domain at the 5' end of the protein. The homology is for a proline-rich conserved domain of nuclear receptor co-activators (PNRC-domain proteins) in single letter amino acid code, present in both invertebrate and vertebrate proteins. Numbers to the left indicate position of the domain within the proteins. (C) Northern blot using two different *aqz* cDNAs as probes reveal three different transcripts of 7.53, 5.0 3 and 3.16 Kb. The smallest band (3.16 Kb) is only present in adult flies, and is only seen using a 5' c DNA (LD47990), present in all *aqz* isoforms. The same blot that was used with the first probe, was photographed, then stripped, and re-probed with the a more 3' cDNA (LD02060), that recognizes *aqz* RB, RC, and RD, but not *aqz* RA. n>10. (D) Aqz mutant and control Western blot using an antibody against GFP recognizes a band at approximately 40 kD (right black

arrow) in *aqz^GFP* homozygotes, and weakly, in *aqz^GFP* heterozygotes. All other weak bands are present in all lanes, including the control, wild type lane, and are, consequently, not specific.
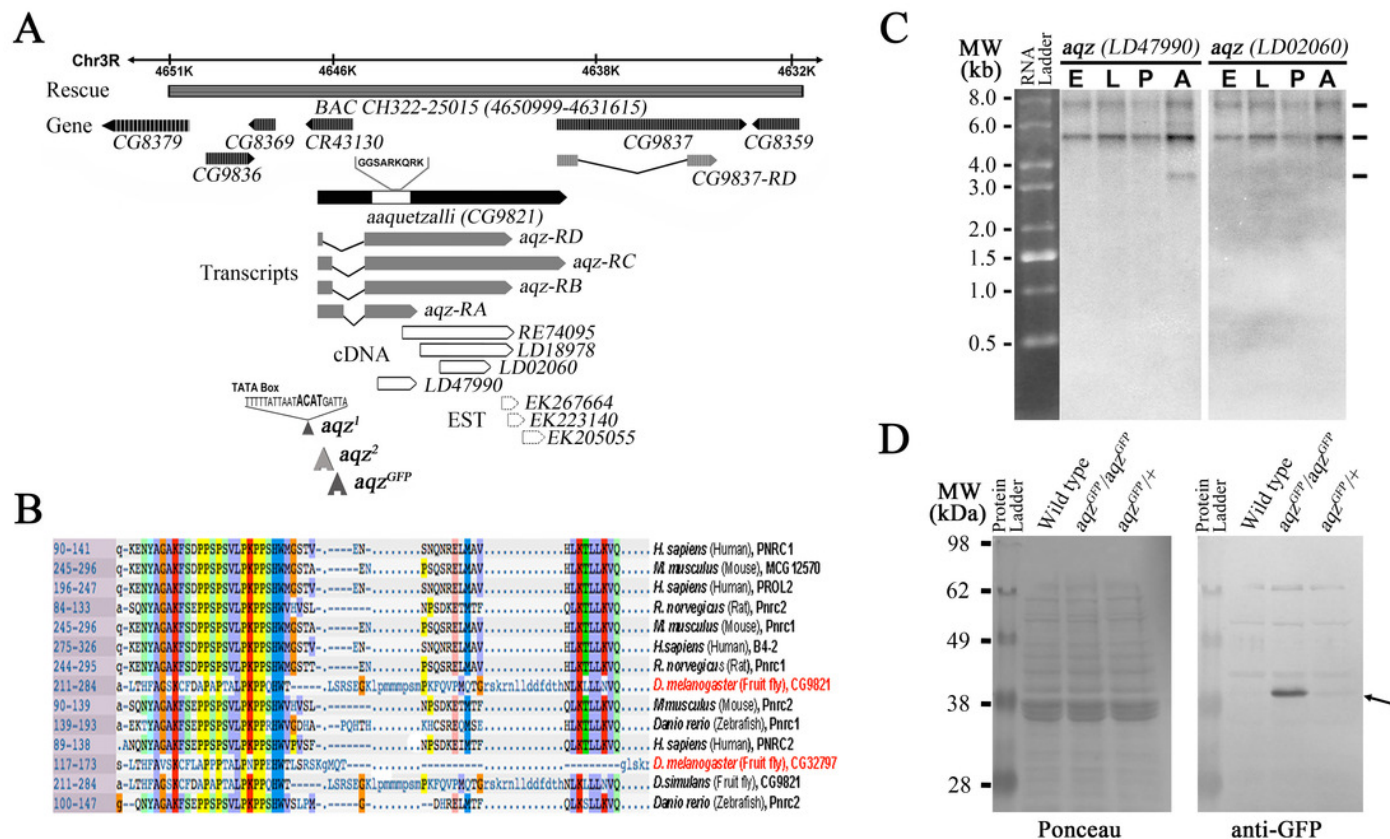
Figure 2

aqz has alterative splicing.

aqz mRNAs first exon is translated, and some have also 3' stop codon read-through in the second exon, judging from ribosome footprinting data. The *aqz* locus (CG9821) together with the annotated predicted mRNAs are depicted on top (green) with dotted lines depicting introns, and red lines depicting other transcripts. The neighboring CG9837 locus, overlapping CG9821 at the 5' end, is also depicted in green. The ribosome footprinting data is depicted below taken from S2 cells (black), 0-2 hrs. embryos (blue) and mRNA-seq (gray) in reads per million. Inset shows a magnification of the Aqz C-terminal region where protein extension may occur.
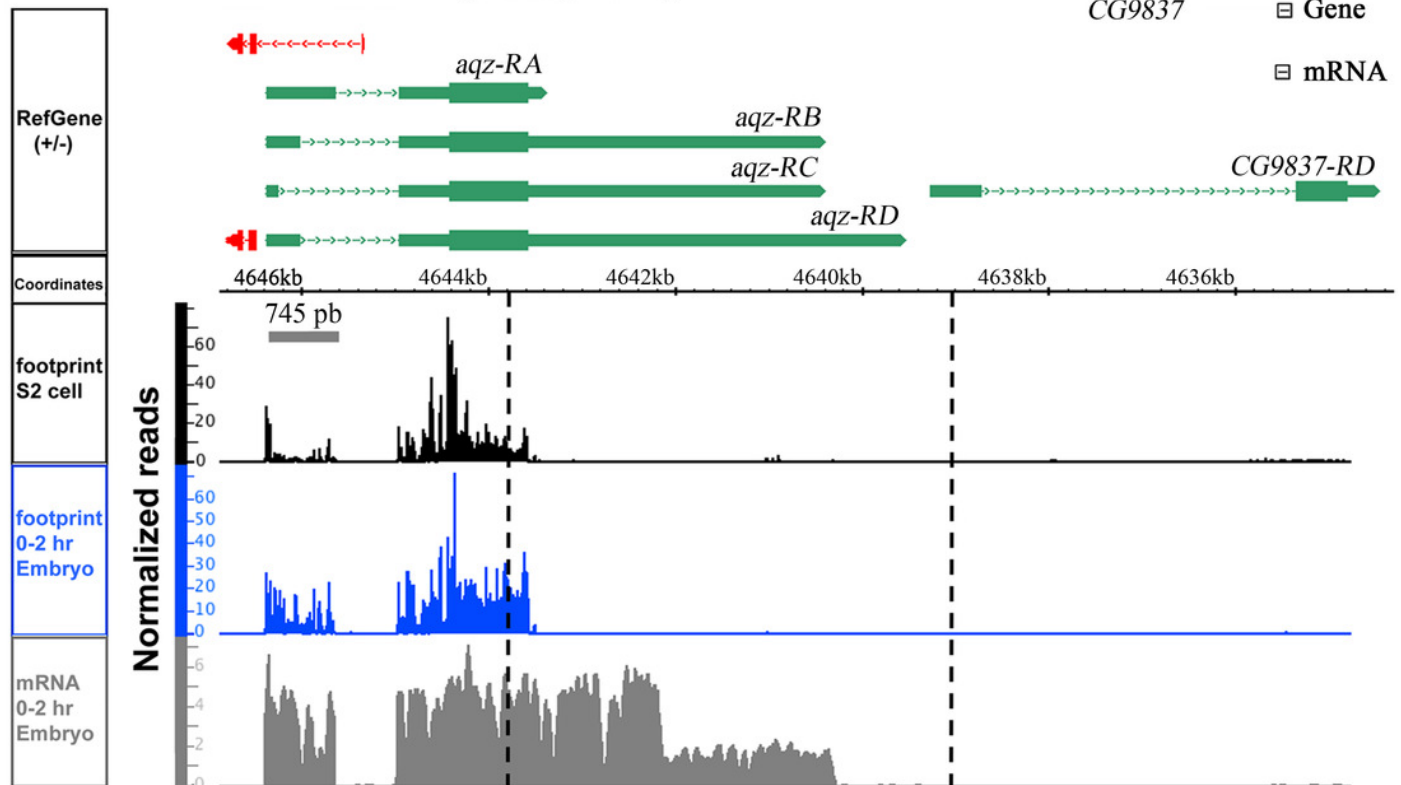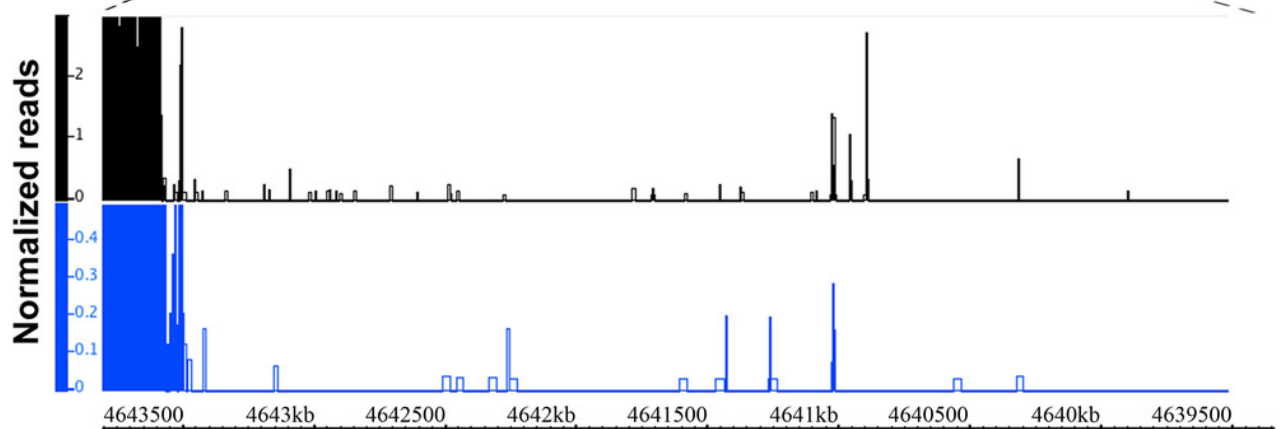
Figure 3

*aqz^GFP*mutant phenotypes

(A) and (B) show mutant (*aqz^GFP/aqz^GFP*) and wild type cuticles, respectively, the former one with an anterior hole and head involution defects (white arrow). (C) and (E) show mutant embryos stained with neuronal and epithelial markers: in (C) anti-Elav for neuronal bodies and anti-Coracle (Cora) for epithelial cells, while in (E) 22C10 for axons and some neuronal bodies. (D) and (F) show the same stainings using wild type control embryos. Scale bar is 100 μm. (G) Shows the percentages of embryos with neural phenotypes in *aqz^GFP/aqz^GFP* embryos, with one or two copies of a genomic rescue construct. One copy of the rescue construct rescues significantly the mutant phenotype, whereas two copies effects a significant, but smaller, rescue, pointing to some gain-of-function effects with two rescue constructs. Two copies of the rescue construct in a wild type background have neurogenic phenotypes in over 40% of embryos, phenotypes similar to *aqz* mutants. In (G) and (H) *aqz^GFP* is homozygous mutant, *aqz^RECUE/+* is one copy of the rescue construct, and *aqz^recue* indicates two copies of the rescue construct. (H) Extended phenocritical period of *aqz^GFP/aqz^GFP* mutants. The surviving *aqz^GFP/aqz^GFP* mutant embryos die majorly as larvae, with approximately 20% reaching pupariation. No adults are ever observed. The *aqz^GFP/aqz^GFP* lethality is rescued to wild type levels with one copy of the *aqz* genomic rescue construct, but two copies of the rescue construct, while having a significant rescue effect, are less effective, pointing to some gain-of-function effects with two rescue constructs. (I) *aqz^GFP/aqz^GFP* mutant pupae die early, with necrosis (left side pupae, black arrow), compared to a control pupae (right side pupae). Scale bar is 1mm. (J) Rescued *aqz^GFP/aqz^GFP* mutant fly (top) compared to sibling control fly (bottom, has curved wings as marker). In this and all figures, ** denotes significant differences. In all figures, for all embryo experiments, representative ones are shown, and n examined is over 200 per condition.
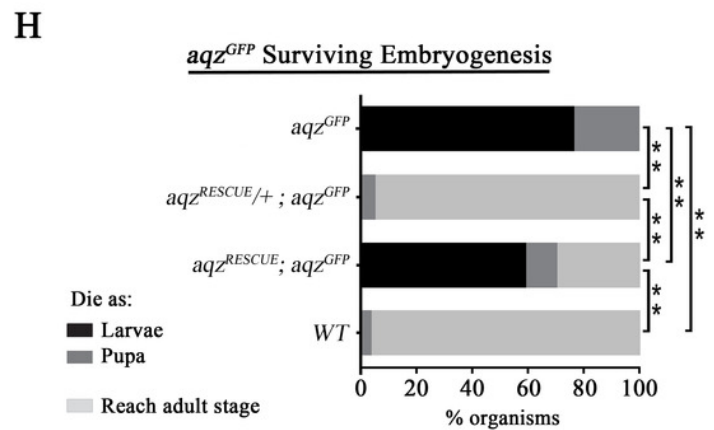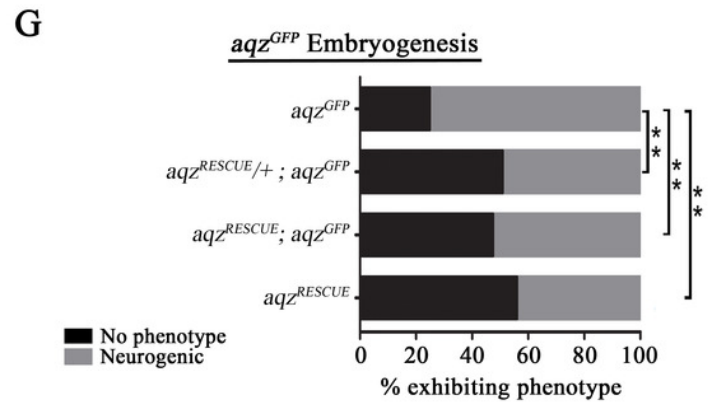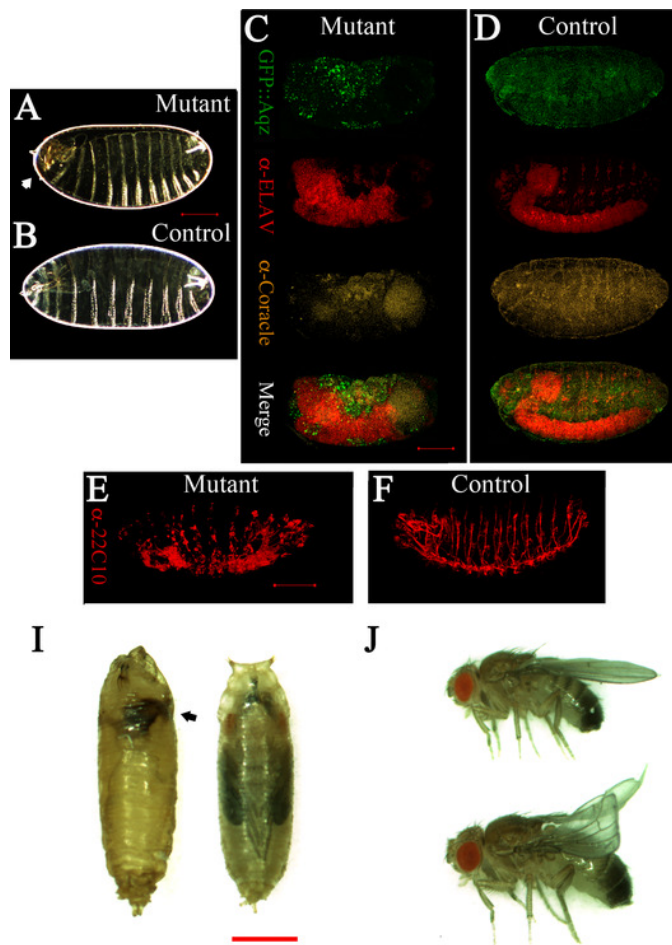
Figure 4

Aqz mRNAs and proteins are expressed throughout embryogenesis in the ectoderm and in ectodermally derived structures, and have maternal contribution.

(A) Anti-sense *aqz in situ* hybridization results at different embryonic stages of development; (B) shows results with the sense control probe (both derived from *aqz* cDNA LD47990). Embryos in (C) are stained with the anti-Aqz antibody, (1:100), whereas (D) shows expression of chimeric GFP::Aqz proteins using an anti GFP antibody (1:100) from the same embryos, which are heterozygous for *aqz^GFP^*, and thus, have expression of both GFP::Aqz and native Aqz protein. As shown in (E), results from both are largely coincidental except some PNS cells and some amnioserosa cells, only labeled with the anti-Aqz antibody. In all panels, anterior is left and dorsal is up. All views are lateral views except the lower row, where ventrolateral views are shown to evidence the developing central nervous system. Stage 5 early syncytial embryo, stage 9-10 germband extension/retraction stages, stage 14 dorsal closure, and stage 17, end of embryogenesis. Scale bar is 100 μm.

Note: Auto Gamma Correction was used for the image. This only affects the reviewing manuscript. See original source image if needed for review.
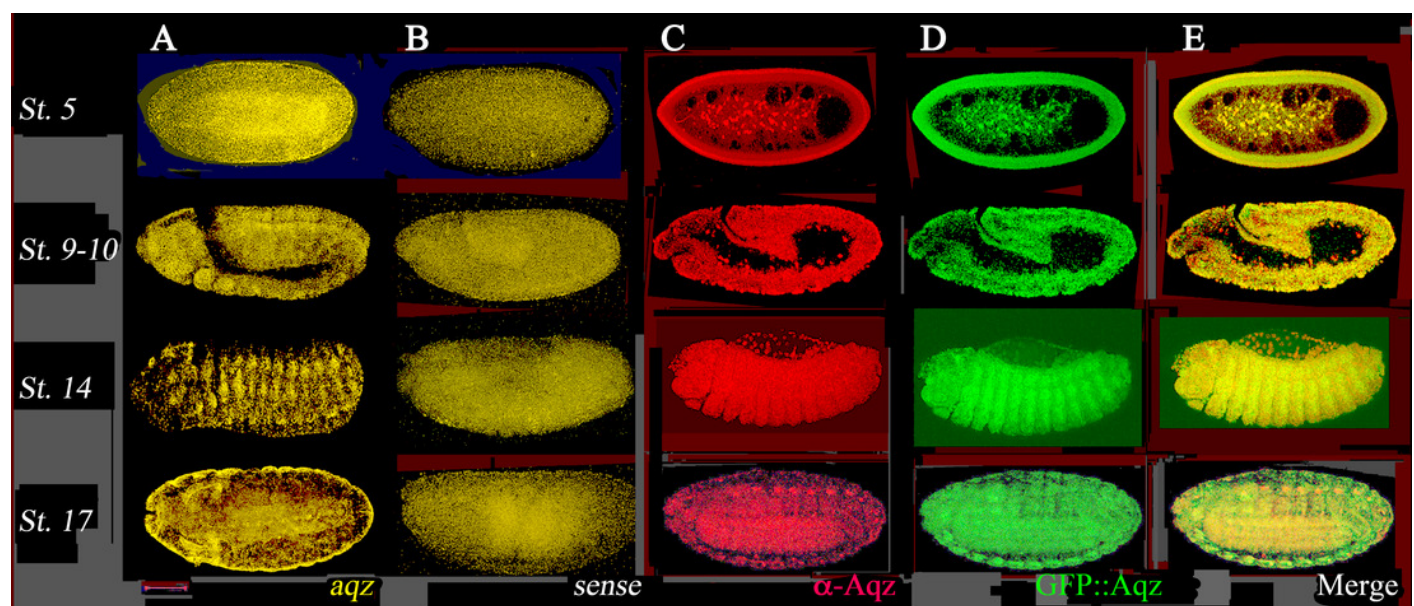
Figure 5

Aqz expressed in ectodermally derived tissue.

Aqz expressed in ectodermally derived tissue. Panel (A) shows an anti-GFP staining for GFP::Aqz expression together with an epidermal marker, anti-Cora, showing some coincidental expression (yellow). For all immune-stainings in the figure, the panels marked underneath the top panels A-D labeled E-F show the GFP::Aqz channel separate, and the panels G-H show the anti-Aqz. The bottom row of panels marked with I, J, K and L depict the anti-coracle (I), anti-Elav (J), anti-22C10 (K), and anti-repo (L) channels, respectively. Panel (B) shows anti-GFP for GFP::Aqz and anti-Elav, to mark neuronal cells in the developing central NS. (C) Using monoclonal 22C10, there is coincidental expression with anti-Aqz antibody, showing that some neurons in the PNS are positive for both Aqz and 22C10 (yellow). (D) In contrast no glial cells (marked by anti-Repo antibody) are coincidental with anti-Aqz antibody staining, showing that glial cells do not express Aqz. Scale bar is 100 µm.

Note: Auto Gamma Correction was used for the image. This only affects the reviewing manuscript. See original source image if needed for review.
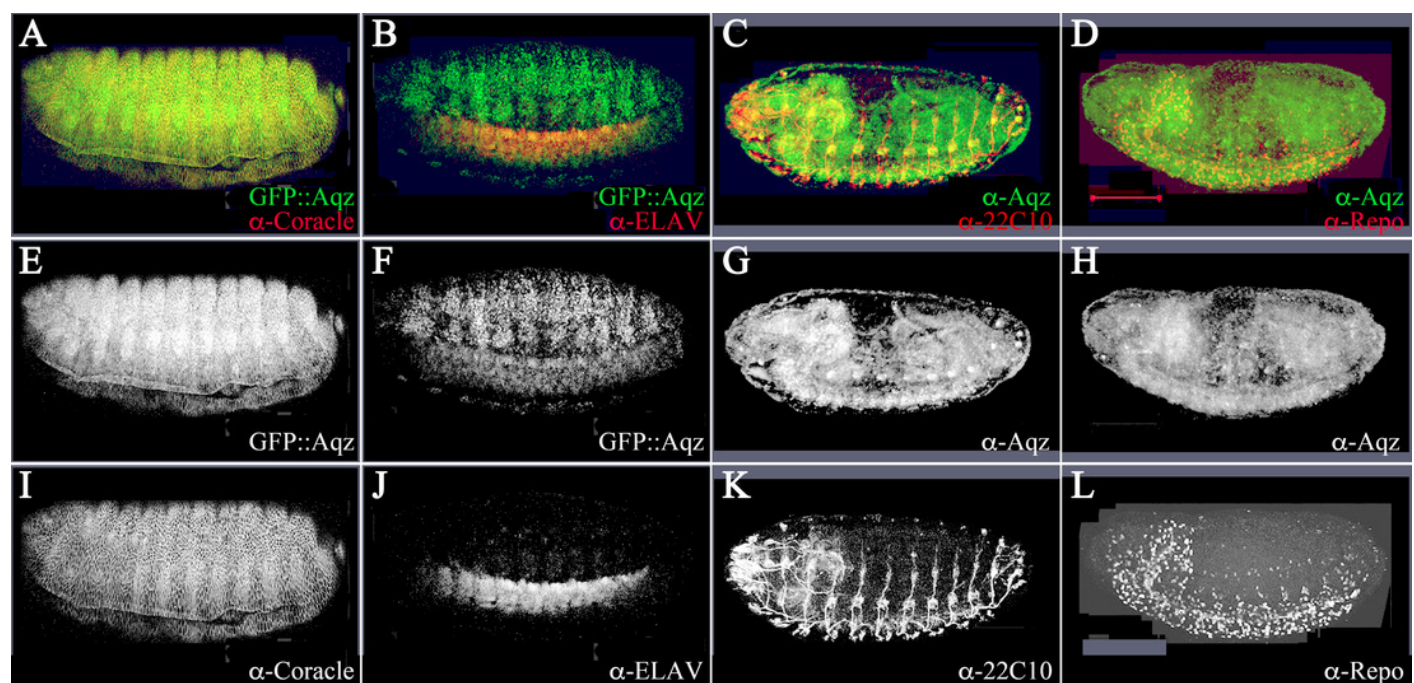
Figure 6

*aqz*NS defects are detected from the onset of NS formation.

aqzNS defects are detected from the onset of NS formation.(A, C, E and G) are *aqz*homozygousmutant embryos stained with markers for the NS. (B, D, F and H) are corresponding heterozygous embryos (controls). All views are lateral with anterior to the left, dorsal up. A and B show anti-Achaete staining marking proneural cell during germband extension/retration. C and D show deadpan marked neuroblasts during germband extension/retraction and condensation of the NS. Notice irregular appearance of neuroblasts in C compared with D (control). E and F show expression of Evenskipped (Eve), marking ganglion mother cells, showing a disruption in the mutant (compare E to F) at this later stage of development (stage 15). G and H mark expression of GFP::Aqz. Green lines underneath G mark parts of the embryo with abnormal GFP::Aqz expression, compared to H, where the GFP::Aqz signal is distributed homogeneously. I marks neuroblasts. They also show a clumped and irregular distribution (compare to J which shows a regular array of neuroblasts). Red lines mark areas with abundant neuroblasts in I. K and L show the merged images. Scale bar is 100 μm.

Note: Auto Gamma Correction was used for the image. This only affects the reviewing manuscript. See original source image if needed for review.
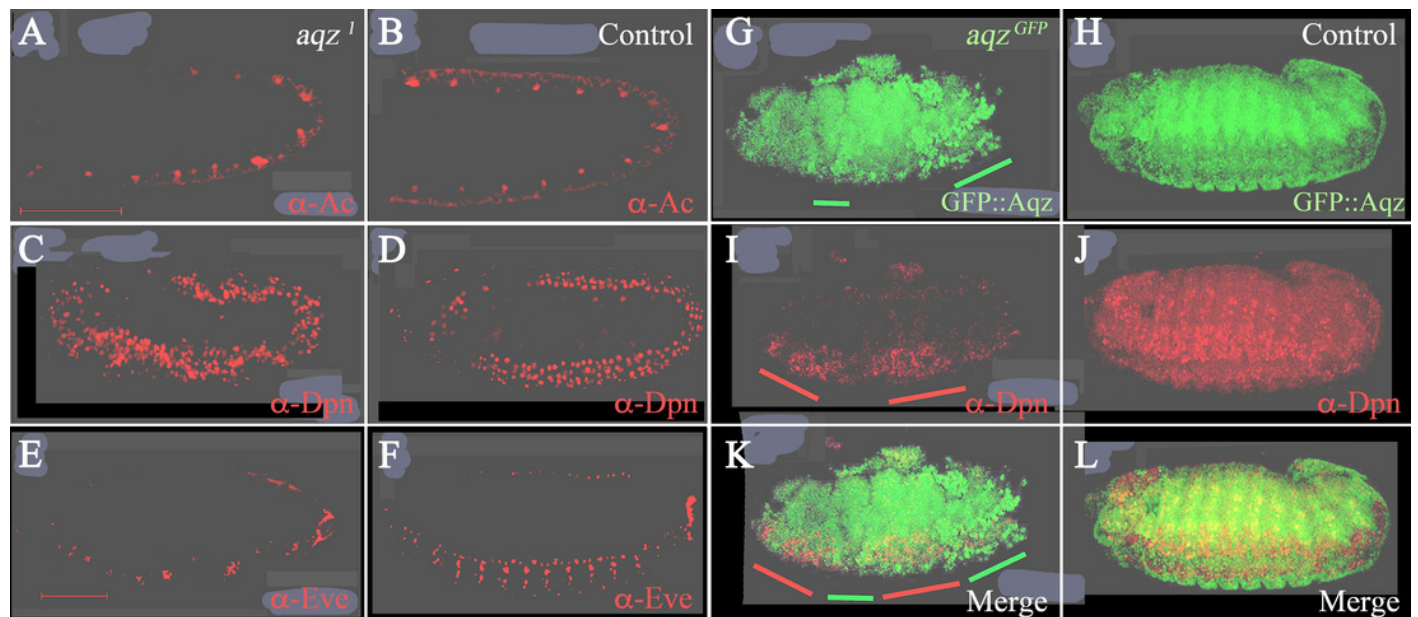
Figure 7

Mutations in Aqz lead to irregular distribution of epithelial tissue and NS.

Mutations in Aqz lead to irregular distribution of epithelial tissue and NS.A and O show lateral views of embryos (anterior to the left and dorsal up) stained for neuroblasts (Deadpan antibodies, red), epithelia (Coracle antibodies, yellow), also showing expression of Aqz (green). Scale bar is 100 μm. In A, two distinct regions showing irregular distribution of labels: A1 and A2, are enclosed in white rectangles and enlarged to the right. For comparison, a similar control area is shown in O, the heterozygous control embryo. B', F and P show enlarged anti-Deadpan staining (red); C, G and Q show enlarged GFP::Aqz expression, D, H and R show enlarged anti-Coracle expression, whilst E, I and S show merged images, respectively. Scale bar is 50 μm.J-N show another example of lack of epithelial cells using a different epidermal marker (anti-FasIII, K) and an irregular distribution of neuroblasts (anti-Deadpan, L) in *aqz^{GFP}*mutant embryos (GFP::Aqz, J). Nuclei are labeled by DAPI (M). N show the respective merged image.
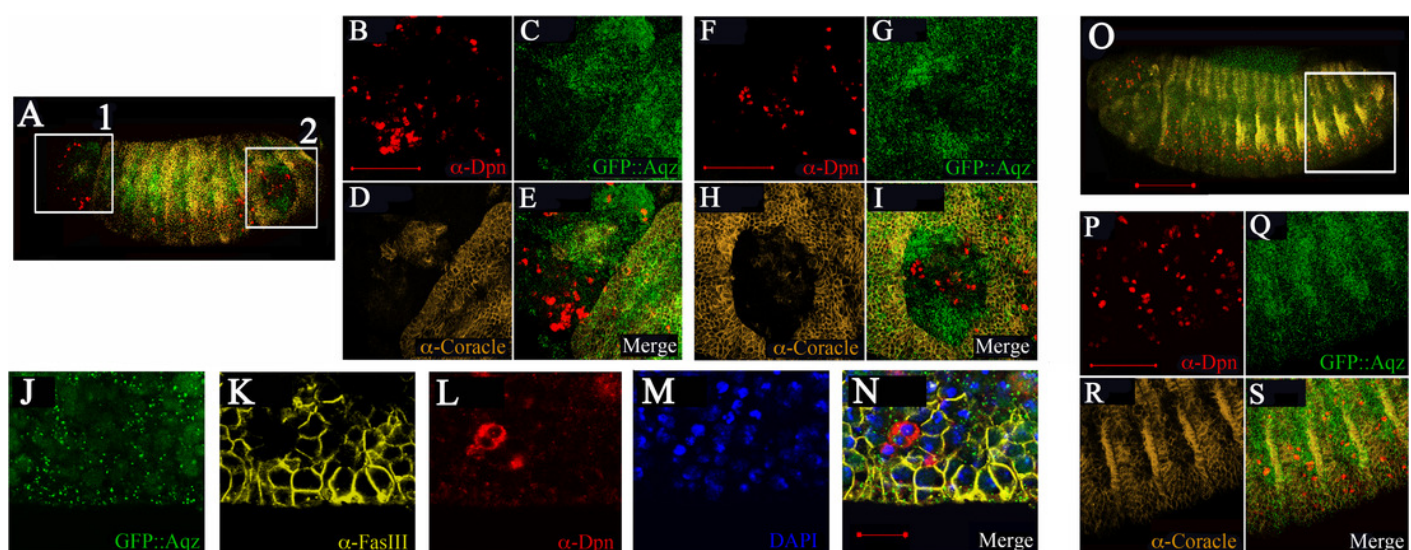
Figure 8

The *aqz* mutant neuroepthelium has polarity defects.

The *aqz* mutant neuroepthelium has polarity defects. A, E, I, M, Q, and U are lateral views of embryos undergoing dorsal closure, with anterior to the left and dorsal up. Bars are 100 μm. A-D, I-L, and Q-T are *aqz^GFP* mutant embryos, whereas E-H, M-P, and U-X are *aqz^GFP* heterozygtes as controls. B, F, J, N, R, and V show GFP::Aqz expression, C and G anti-Crumbs (Crb) (red), K and O anti-Discs large (Dlg) (red), and S and W anti-Delta (Dl) (yellow). D, H, L, and P show respective merged images. Scale bar is 50 μm. T and X show anti-DE-cadherin (DE-Cad) (red). Note that homozygous mutant GFP::Aqz expression appears more clumped compared to the heterozygous controls, as stated before, and aids in identification of mutant embryos.

Note: Auto Gamma Correction was used for the image. This only affects the reviewing manuscript. See original source image if needed for review.